

Sparsity-Constraint Optimization via Splicing Iteration

Ze zhi Wang^{*}, Borui Tang, Xueqin Wang[†]

International Institute of Finance, School of Management, University of Science and Technology of China, homura@mail.ustc.edu.cn, tangborui@mail.ustc.edu.cn, wangxq20@ustc.edu.cn

Jin Zhu^{*}

Department of Statistics, London School of Economics and Political Science, xJ.Zhu69@lse.ac.uk

Junxian Zhu^{*}

Saw Swee Hock School of Public Health, National University of Singapore, junxian@nus.edu.sg

Hongmei Lin[†]

School of Statistics and Information, Shanghai University of International Business and Economics, hmlin@suibe.edu.cn

Abstract. Sparsity-constraint optimization has wide applicability in signal processing, statistics, and machine learning. Existing fast algorithms must burdensomely tune parameters, such as the step size or the implementation of precise stop criteria, which may be challenging to determine in practice. To address this issue, we develop an algorithm named sparsity-constraint optimization via splicing iteration (SCOPE) to optimize nonlinear differential objective functions with strong convexity and smoothness in low dimensional subspaces. Algorithmically, the SCOPE algorithm converges effectively without tuning parameters. Theoretically, SCOPE has a linear convergence rate and converges to a solution that recovers the true support set when it correctly specifies the sparsity. We also develop parallel theoretical results without restricted-isometry-property-type conditions. We apply SCOPE’s versatility and power to solve sparse quadratic optimization, learn sparse classifiers, and recover sparse Markov networks for binary variables. The numerical results on these specific tasks reveal that SCOPE perfectly identifies the true support set with a 10–1000 speedup over the standard exact solver, confirming SCOPE’s algorithmic and theoretical merits. Our open-source Python package `scope` based on C++ implementation is publicly available on GitHub, reaching a ten-fold speedup on the competing convex relaxation methods implemented by the `cvxpy` library.

Key words: sparsity-constrained optimization, support recovery, linear convergence rate, splicing technique

1. Introduction

This paper aims to develop an algorithm to solve the sparsity-constrained optimization:

$$\arg \min_{\boldsymbol{\theta} \in \mathbb{R}^p} f(\boldsymbol{\theta}), \text{ s.t. } \|\boldsymbol{\theta}\|_0 \leq s, \quad (1)$$

where $f : \mathbb{R}^p \rightarrow \mathbb{R}$ is a differentiable objective function with strong convexity and smoothness in low dimensional subspaces, $\boldsymbol{\theta}$ is a p -dimensional parameter vector, $\|\boldsymbol{\theta}\|_0$ is the ℓ_0 -norm that counts the non-zero coordinates in $\boldsymbol{\theta}$, and s is a given integer controlling the sparsity of the solution of (1).

As an interesting topic in optimization (Beck and Eldar 2013), problem (1) acquires increasing significance in machine learning, statistics, and signal processing nowadays, in which it also refers to the sparsity

^{*} Equal contribution

[†] Corresponding author

learning or subset selection. We exemplify with compressive sensing that aims to recover a sparse signal vector $\boldsymbol{\theta} \in \mathbb{R}^p$, which is formulated as:

$$\arg \min_{\boldsymbol{\theta} \in \mathbb{R}^p} \|\mathbf{y} - \mathbf{X}\boldsymbol{\theta}\|_2^2, \text{ s.t. } \|\boldsymbol{\theta}\|_0 \leq s, \quad (2)$$

where $\|\cdot\|_2$ is the ℓ_2 -norm, $\mathbf{y} \in \mathbb{R}^n$ are the observations, $\mathbf{X} \in \mathbb{R}^{n \times p}$ is the sensing matrix. Although problem (2) has received extensive studies (see, e.g., Donoho 2006, Tropp and Gilbert 2007, Blumensath and Davies 2008, Needell and Tropp 2009, Foucart 2011), the study of (1) is still limited because of the flexibility of the objective function. Even more difficult, the constraint function is non-convex, and in fact, is non-continuous, rendering problem (1) quite challenging.

1.1. Literature review

We roughly categorize the main existing methods for (1) into two categories: hard thresholding (HT) based methods and searching-based methods.

The HT-based algorithms leverage the information of the sparsity s and use the HT operators to produce an s -sparse solution. As one of the most classical HT-based algorithms, iterative hard thresholding (IHT) was first proposed by Blumensath and Davies (2008) under quadratic objective function and was extended to more general objective functions (Beck and Eldar 2013, Jain et al. 2014, Zhu et al. 2022). Bahmani et al. (2013) proposed the gradient support pursuit (GraSP), which is another classical HT-based method for (1). Despite the powerful numerical performance, the above two HT-type methods lack a theoretical guarantee for recovering the true support set. The gradient hard thresholding pursuit (GraHTP, Yuan et al. (2017)) improves IHT by additionally conducting a debias step on the s -sparse solution in each iteration. Although it enjoys support-set recovery and convergence under certain conditions, these properties both depend on a continuous hyperparameter that may not be easy to choose in practice (see the remark following Theorem 1). The Newton hard thresholding pursuit (NHTP, Zhou et al. (2021)) replaces the debias step in GraHTP with a Newton step to accelerate its convergence. Yet, NHTP still needs to choose a similar hyperparameter in GraHTP. Wen et al. (2020) overcame the hardness of selecting continuous hyperparameters in GraHTP, but their method has no theoretical justification. The dual IHT (DIHT, Yuan et al. (2020)) is a recently proposed IHT-style method that executes the HT operator on the dual problem. Unfortunately, DIHT only works for objective functions comprising a ℓ_2 -penalty for $\boldsymbol{\theta}$.

The searching-based methods seek a coordinate set that can minimize $f(\cdot)$. The most direct method is to enumerate all possible coordinate sets with cardinality s . This method yields an exact solution, yet it has a heavy computational burden. Another approach reformulates (1) as a mixed integer optimization (MIO) problem and then searches for the optimal solution of the MIO problem with the off-the-shelf solvers (Bertsimas et al. 2021). Nevertheless, this approach still has a sharply increasing runtime concerning dimension p , and Shalev-Shwartz et al. (2010) suggested a greedy method instead. The greedy method iteratively

appends one important coordinate with the largest gradient magnitude at the current solution. Then it derives a new solution by minimizing $f(\cdot)$ over selected coordinates. This iteration repeats until s coordinates are collected. However, this algorithm cannot remove the wrong coordinates selected in early iterations. To address this issue, Liu et al. (2014) proposed a forward-backward greedy algorithm. Specifically, after choosing an important coordinate in each iteration, the greedy algorithm may drop some coordinates with a tiny contribution to the objective function to correct previous mistakes. Unfortunately, the threshold of tiny contribution is a continuous tuning parameter that is hard to tune (Liu et al. 2014). Another computationally efficient searching-based method leverages the current solution to derive a better solution through the local swapping of coordinates (Zhu et al. 2020, Hazimeh and Mazumder 2020). In particular, Zhu et al. (2020) proved that, for linear models, a few iterations of local swapping could select the true support set under certain conditions.

1.2. Our Proposal and Contribution

This paper aims to develop a computationally efficient algorithm with a provably accurate solution for problem (1). To this end, we propose a new iterative algorithm, the sparsity-constrained optimization via splicing iteration (SCOPE). At each iteration, SCOPE leverages zeroth-order and first-order information at the current solution and performs local swapping to overcome the challenges of general objective functions and the sparsity constraint. Besides, in each iteration, SCOPE exploits the objective values to guide the local swapping to ensure the objective value monotonously decreases with the number of iterations; in conjunction with the fact that support sets with cardinality s are finite, SCOPE must converge without carefully setting continuous tuning parameters to reach convergence. This is a distinctive feature of SCOPE.

The main contribution of this article is as follows:

1. We propose a novel iterative algorithm, the SCOPE, to solve (1). It is attractive in practice because it is tuning-free and can naturally converge. More importantly, under certain conditions, theoretical analysis guarantees SCOPE correctly identifies the true support set and gives an optimal solution. Notably, this property can be reached without tuning parameters.
2. The convergence analysis shows that, under the same conditions, SCOPE is computationally efficient because it has a linear convergence rate. Upon this, we explicitly deduce the number of iterations required to recover the true support set, which is much smaller than the enumeration. Furthermore, we prove that the solutions within algorithmic iterations geometrically converge to the ground truth.
3. Moreover, we have demonstrated that, even when the restricted isometry property (RIP) type conditions are absent, the algorithm can still accurately identify the true support set by relaxing sparsity. We again established the linear convergence rate in this scenario, along with similar computational properties mentioned earlier.

4. We apply SCOPE to three benchmarked concrete sparse-constrained optimization problems. With our open-source Python/C++ library in Github (<https://github.com/abess-team/skscope>), SCOPE often perfectly selects the support set like the MIO solver but consumes a significantly shorter runtime. The comparisons against state-of-the-art methods reveal SCOPE uses fewer sample sizes to correctly identify the support set and typically achieves a 10-fold acceleration compared to competing methods.

1.3. Notations

We summarize some notations for the content below. In the following, bold lowercase letters (e.g., $\mathbf{x}, \boldsymbol{\theta}$) represent vectors, while bold uppercase letters (e.g., \mathbf{X}, \mathbf{Y}) represent matrices. Let $I(\cdot)$ be the indicator function, $[p]$ be $\{1, 2, \dots, p\}$, and \mathcal{A}, \mathcal{B} be subsets of $[p]$.

- $\boldsymbol{\theta}^*$: the ground truth s -sparse parameter vector.
- $\|\mathbf{x}\|_2$: the Euclidean norm of \mathbf{x} . In many times, we also use $\|\mathbf{x}\|$ to denote $\|\mathbf{x}\|_2$.
- $\|\mathbf{x}\|_0$: the number of non-zero elements of \mathbf{x} .
- $\|\mathbf{x}\|_\infty$: the maximum absolute value of \mathbf{x} .
- $\text{supp}(\mathbf{x})$: the support set of \mathbf{x} , i.e., $\text{supp}(\mathbf{x}) = \{j \mid \mathbf{x}_j \neq 0\}$. In particular, denote $\mathcal{A}^* := \text{supp}\{\boldsymbol{\theta}^*\}$.
- $\text{diag}\{\mathbf{x}\}$: a diagonal matrix with \mathbf{x} as its diagonal element.
- $\mathcal{H}_t(\cdot)$: a $\mathbb{R}^p \rightarrow \mathbb{R}^p$ mapping that keeps the t elements with the largest magnitude and sets the rest to zero.
- $\nabla f(\mathbf{x})$: the gradient of $f(\cdot)$ at \mathbf{x} .
- $\nabla^2 f(\mathbf{x})$: the Hessian matrix of $f(\cdot)$ at \mathbf{x} .
- $|\mathcal{A}|$: the cardinality of the set \mathcal{A} .
- $\mathbf{x}_{\mathcal{A}}$: a $\mathbb{R}^{|\mathcal{A}|}$ -dimensional sub-vector of \mathbf{x} containing coordinates on \mathcal{A} .
- $\mathbf{x}|_{\mathcal{A}}$: a vector whose the j coordinate equal to \mathbf{x}_j if $j \in \mathcal{A}$ else zero.
- $\mathbf{X}_{\mathcal{A}}$: the sub-matrix of \mathbf{X} consisting of columns on \mathcal{A} .
- $\mathbf{X}_{\mathcal{A}, \cdot}$: the sub-matrix of \mathbf{X} consisting of rows on \mathcal{A} .
- $\mathbf{X}_{\mathcal{A}, \mathcal{B}}$: the sub-matrix of \mathbf{X} consisting of rows on \mathcal{A} and columns on \mathcal{B} .
- $\nabla_{\mathcal{A}} f(\mathbf{x})$: it is identical to $(\nabla f(\mathbf{x}))_{\mathcal{A}}$.
- $\nabla_{\mathcal{B}} \nabla_{\mathcal{A}} f(\mathbf{x})$: is equal to $((\nabla^2 f(\mathbf{x}))_{\mathcal{A}, \cdot})_{\mathcal{B}}$. Particularly, denote $\nabla_{\mathcal{A}}^2 f(\mathbf{x}) := \nabla_{\mathcal{A}} \nabla_{\mathcal{A}} f(\mathbf{x})$.

1.4. Organization

The rest of this article is organized as follows. We first present a new iterative algorithm, the SCOPE, in Section 2. Then, we illustrate the theoretical properties of SCOPE on the solution and computation in Section 3, and the main proofs of these properties are given in Section 4. The applications of SCOPE on three specific tasks are discussed in Section 5, followed by Section 6 that studies the numerical performance of SCOPE on these tasks. Finally, we conclude this article in Section 7.

2. Algorithm

The fundamental motivation of our algorithm is to improve upon the current support solution and derive a new solution with better quality. To rephrase, we expect to generate a sequence of solutions: $\mathcal{A}^0, \mathcal{A}^1, \dots \subseteq [p]$ from an arbitrary guess \mathcal{A}^0 , and pick out the last one in the sequence as the algorithmic solution. Suppose \mathcal{A}^t is the t -th solution and $|\mathcal{A}^t| = s$, a heuristic idea to improve upon \mathcal{A}^t is replacing some irrelevant elements in \mathcal{A}^t with the same number of top relevant elements in $\mathcal{I}^t := (\mathcal{A}^t)^c$, where the concept of “relevance” can be measured by the decrease of the objective function. Zhu et al. (2020) refer to this idea as “splicing” and derives an easy-to-compute criterion for quantitatively measuring the concept of relevance under the linear models. However, deriving a criterion for relevance is much more challenging for diverse objective functions because it should simultaneously satisfy: (P1) the adaptation of diverse objective functions and (P2) high computational efficiency.

Here, we give a new criterion that enjoys (P1) and (P2) mentioned above. To this end, we define the relevance as:

$$\xi_j^t \propto \begin{cases} (\theta_j^t)^2, & j \in \mathcal{A}^t \\ [\nabla_j f(\theta^t)]^2, & j \in \mathcal{I}^t \end{cases}, \quad (3)$$

where $\theta^t := \arg \min_{\text{supp}\{\theta\}=\mathcal{A}^t} f(\theta)$ is the current solution under \mathcal{A}^t . The rationale behind the relevance is easy to grasp: for $j \in \mathcal{A}^t$, the element with a larger parameter magnitude is more relevant; for $j \in \mathcal{I}^t$, a larger magnitude on gradient implies adding this element has a greater potential to decrease the objective value, and thus, it shall be more relevant. Moreover, from Equation (3), the relevance satisfies (P1) because it applies to differentiable objective functions. Finally, Equation 3 can be easily computed, thus satisfying (P2). To see that, we emphasize that Equation (3) is a closed-form expression with respect to θ^t and $\nabla f(\theta^t)$. Among them, θ^t can be obtained by optimizing objective function in a low dimensional parameter space since only s parameters have non-zero values; as for $\nabla f(\theta^t)$, their expressions can be easily obtained.

Now we depict the splicing procedure with the relevance defined in Equation (3). Specifically, suppose we would like to swap k elements of \mathcal{A}^t and \mathcal{I}^t , then coordinates to be swapped are:

$$\begin{aligned} \mathcal{S}_{\mathcal{A}}^{(k)} &= \{j \in \mathcal{A}^t : \xi_j^t \text{ is in the smallest } k \text{ of } \{\xi_j^t\}_{j \in \mathcal{A}^t}\}, \\ \mathcal{S}_{\mathcal{I}}^{(k)} &= \{j \in \mathcal{I}^t : \xi_j^t \text{ is in the largest } k \text{ of } \{\xi_j^t\}_{j \in \mathcal{I}^t}\}. \end{aligned} \quad (4)$$

Notice that, it might be possible that $|\mathcal{S}_{\mathcal{A}}^{(k)}|$ or $|\mathcal{S}_{\mathcal{I}}^{(k)}|$ is not equal to k because ξ_j^t has the same value. Although this extreme case would not appear in the application in this paper, one possible solution for this case is to randomly choose some of them to ensure $|\mathcal{S}_{\mathcal{A}}^{(k)}| = |\mathcal{S}_{\mathcal{I}}^{(k)}| = k$. And then, the splicing generates a candidate active set $\tilde{\mathcal{A}}^{(k)} := (\mathcal{A}^t \setminus \mathcal{S}_{\mathcal{A}}^{(k)}) \cup \mathcal{S}_{\mathcal{I}}^{(k)}$ with cardinality s and evaluates it by the objective function under $\tilde{\mathcal{A}}^{(k)}$, i.e., $\tilde{f}^{(k)} := \min_{\text{supp}\{\theta\}=\tilde{\mathcal{A}}^{(k)}} f(\theta)$. Consider all possible $k \in \{1, \dots, s\}$ and find $k^* := \arg \min_{k \in [s]} \tilde{f}^{(k)}$, if $\tilde{f}^{(k^*)} < f(\theta^t)$, then we believe that $\tilde{\mathcal{A}}^{(k^*)}$ is superior to \mathcal{A}^t and we should accept this spliced set by $\mathcal{A}^{t+1} \leftarrow \tilde{\mathcal{A}}^{(k^*)}$. If $\tilde{f}^{(k^*)} > f(\theta^t)$, no candidate active set is better than \mathcal{A}^t , then we set \mathcal{A}^t as the algorithmic output. We summarize the splicing procedure depicted above in Algorithm 1.

Algorithm 1: Sparsity-Constrained Optimization via Splicing Iteration (SCOPE)**Input:** An initial active set \mathcal{A}^0 with cardinality s and the maximum splicing size $k_{\max}(\leq s)$.**Result:** $(\boldsymbol{\theta}^t, \mathcal{A}^t)$.

```

1 Initialize:  $t \leftarrow -1, \mathcal{I}^0 \leftarrow (\mathcal{A}^0)^c, \boldsymbol{\theta}^0 \leftarrow \arg \min_{\text{supp}\{\boldsymbol{\theta}\}=\mathcal{A}^0} f(\boldsymbol{\theta})$ .
2 repeat // Splicing Iteration
3    $t \leftarrow t + 1, \mathcal{A}^t \leftarrow \mathcal{A}^{t-1}, \boldsymbol{\theta}^t \leftarrow \boldsymbol{\theta}^{t-1}$ , and  $L \leftarrow f(\boldsymbol{\theta}^t)$ .
4   Update the relevance of each coordinate via Equation (3).
5   for  $k = 1$  to  $k_{\max}$  do // Splicing Operator
6     Select the  $k$  coordinates  $\mathcal{S}_{\mathcal{A}}^{(k)}, \mathcal{S}_{\mathcal{I}}^{(k)}$  that to be swapped via Equation (4).
7     Update  $\tilde{\mathcal{A}}^{(k)} \leftarrow (\mathcal{A}^t \setminus \mathcal{S}_{\mathcal{A}}^{(k)}) \cup \mathcal{S}_{\mathcal{I}}^{(k)}$  and solve  $\tilde{\boldsymbol{\theta}}^{(k)} \leftarrow \arg \min_{\text{supp}\{\boldsymbol{\theta}\}=\tilde{\mathcal{A}}^{(k)}} f(\boldsymbol{\theta})$ .
8     if  $L > f(\tilde{\boldsymbol{\theta}}^{(k)})$  then
9        $(L, \mathcal{A}^{t+1}, \boldsymbol{\theta}^t) \leftarrow (f(\tilde{\boldsymbol{\theta}}^{(k)}), \tilde{\mathcal{A}}^{(k)}, \tilde{\boldsymbol{\theta}}^{(k)})$ .
10    end
11  end
12 until  $\mathcal{A}^{t+1} = \mathcal{A}^t$ ;

```

REMARK 1. SCOPE incorporates the idea of splicing, but it is not a direct generalization of Zhu et al. (2020) due to two notable differences. Firstly, SCOPE does not use the relevance defined in Zhu et al. (2020), such as $f(\boldsymbol{\theta}^t) - \min_{\text{supp}\{\boldsymbol{\alpha}\}=\{j\}} f(\boldsymbol{\theta}^t + \boldsymbol{\alpha})$ for each $j \in \mathcal{I}^t$, which is computationally expensive since plenty of univariate optimization problems have to be solved. Secondly, in each splicing iteration, SCOPE searches for the best spliced set among $\{\tilde{\mathcal{A}}^{(1)}, \dots, \tilde{\mathcal{A}}^{(k_{\max})}\}$ that is associated with the smallest objective. In contrast, Zhu et al. (2020) accepts a spliced set once it reduces the objective. This difference leads to larger objective deductions at each splicing iteration in SCOPE, ensuring the linear convergence rate of SCOPE (see Theorems 2 and 5).

REMARK 2. For the active set sequence $\mathcal{A}^0, \mathcal{A}^1, \dots$, generated in Algorithm 1, it must have a terminal \mathcal{A}^T where T is a finite integer. It means Algorithm 1 naturally converges without imposing any assumption. The reason is that objective function values are monotonously decreasing, and there are finite s -cardinality subsets of $[p]$.

REMARK 3. Our theoretical analysis indicates that the quality of the initial activation set \mathcal{A}^0 only affects the minimum number of iterations. Still, it does not affect the convergence rate of Algorithm 1. Naturally, a good initial guess \mathcal{A}^0 must accelerate the convergence. To achieve fast convergence, we choose \mathcal{A}^0 in the following manner. Let $\xi_j^0 = [\nabla_j f(\mathbf{0})]^2$ for $j = 1, \dots, p$, we set $\mathcal{A}^0 \leftarrow \{j \mid |\xi_j^0| \geq \bar{\xi}\}$, where $\bar{\xi}$ is the s -largest element among $\{|\xi_1^0|, |\xi_2^0|, \dots, |\xi_p^0|\}$.

REMARK 4. The maximum splicing size k_{\max} is a tuning-free discrete hyperparameter. From the proof of the theoretical results, setting $k_{\max} = s$ guarantees SCOPE has a high-quality solution and computa-

tional properties, so a natural choice for k_{\max} is s . This leads to a tuning-free algorithm, which is used for numerical experiments in Section 6. Additional discussion about k_{\max} is defer to Appendix C.

3. Algorithmic Properties

This section will present solution guarantees and convergence analysis for the algorithm in Sections 3.2 and 3.3, together with high-level proof for the core ones. Before presenting these guarantees, we show assumptions and necessary discussions in Section 3.1. To avoid the RIP-type condition mentioned in Section 3.1, we relax the sparsity level and attain properties on the solution and computation in Section 3.4.

3.1. Assumptions

Our first assumption is related to the convexity and smoothness of the objective function in the subspace. Before the first assumption, we introduce the concepts of restricted strong convexity (RSC) and restricted strong smoothness (RSS) below.

DEFINITION 1 (RESTRICTED STRONG CONVEXITY AND RESTRICTED STRONG SMOOTHNESS). Let t be a positive integer, we say function $f(\cdot)$ is m_t -RSC if

$$\frac{m_t}{2} \|\mathbf{x} - \mathbf{y}\|_2^2 + \langle \nabla f(\mathbf{y}), \mathbf{x} - \mathbf{y} \rangle \leq f(\mathbf{x}) - f(\mathbf{y}),$$

for any $\mathbf{x}, \mathbf{y} \in \mathbb{R}^p$ satisfying $\|\mathbf{x} - \mathbf{y}\|_0 \leq t$. And say $f(\cdot)$ is M_t -RSS if

$$f(\mathbf{x}) - f(\mathbf{y}) \leq \frac{M_t}{2} \|\mathbf{x} - \mathbf{y}\|_2^2 + \langle \nabla f(\mathbf{y}), \mathbf{x} - \mathbf{y} \rangle,$$

for any $\mathbf{x}, \mathbf{y} \in \mathbb{R}^p$ satisfying $\|\mathbf{x} - \mathbf{y}\|_0 \leq t$.

In a geometric sense, a m_t -RSC and M_t -RSS function $f(\cdot)$ possess strong convexity and strong smoothness in any low-dimensional subspace with a dimension less than t . To rephrase, m_t -RSC and M_t -RSS bound the curvature of f in low-dimensional subspaces. With the definition of RSC and RSS, the first assumption is given as follows:

ASSUMPTION 1. $f(\cdot)$ is m_{3s} -RSC and M_{3s} -RSS.

This assumption only requires $f(\cdot)$ to be strong convex and smooth in subspaces, which is much weaker than the convexity and smoothness in the full space. Thus, in Algorithm 1, the optimization problem in subspaces (Lines 1 and 7 in Algorithm 1) always has a unique minimizer, ensuring that Algorithm 1 can properly work. More importantly, it is critical for theoretical analysis because it paves the way for bounding $f(\boldsymbol{\theta}) - f(\boldsymbol{\theta}^*)$, where $\boldsymbol{\theta}$ is a s -sparse solution whose support set may be incorrect. Actually, Assumption 1 is widely used in literature for the studies of algorithms for general sparse-constrained optimization problems (Jain et al. 2014, Yuan et al. 2017, Zhou et al. 2021). This concept is similar to the restricted isometry property in the field of compressed sensing (Candes and Tao 2005), where a quadratic objective function is involved. Assumption 1 serves as its extension for adaptation of general objective functions.

Next, we turn to the second assumption. For unconstrained optimization, $\nabla f(\boldsymbol{\theta}^*) = \mathbf{0}$ is a necessary condition for $\boldsymbol{\theta}^*$ to be a local minimizer of $f(\cdot)$. Here, we relax the zero gradient condition for $\boldsymbol{\theta}^*$ to a weaker one. Let $\vartheta := \min_{j \in \mathcal{A}^*} |\boldsymbol{\theta}_j^*|$, and our assumption is given as follows:

ASSUMPTION 2. $\|\nabla f(\boldsymbol{\theta}^*)\|_\infty \leq \frac{0.35}{\sqrt{s}}(1.49m_{3s} - M_{3s})\vartheta$.

$\|\nabla f(\boldsymbol{\theta}^*)\|_\infty$ in this Assumption can be interpreted as the magnitude of noise. In the noiseless setting, $\|\nabla f(\boldsymbol{\theta}^*)\|_\infty = 0$; while the noise is non-negligible, $\|\nabla f(\boldsymbol{\theta}^*)\|_\infty$ would be a positive value (see Section 5 for concrete examples). From intuition, the noise should not be too large to submerge the signal of true parameters. Assumption 2 expresses this intuitive idea by controlling $\nabla f(\boldsymbol{\theta}^*)$ with the minimum signal of parameters. Such an assumption makes our analyses are applicable to the noised systems that frequently appear in the field of data science. And thus, similar assumptions for $\|\nabla f(\boldsymbol{\theta}^*)\|_\infty$ are widely imposed for sparsity constraint optimization (Bahmani et al. 2013, Yuan et al. 2017). Notice that the upper bound in this assumption implicitly comprises two restrictions for $f(\cdot)$. First, it requires $\|\nabla f(\boldsymbol{\theta}^*)\|_\infty$ in Assumption 2 cannot grow too fast with respect to s ; more precisely, it should be $\mathcal{O}(s^{-\frac{1}{2}})$ which has the same order as Yuan et al. (2017). Second, it requires the so-called restrict condition number $\frac{M_{3s}}{m_{3s}}$ to be upper bounded, which is essentially a RIP-type condition (Candes et al. 2006, Needell and Tropp 2009). We would like to note that $\frac{M_{3s}}{m_{3s}} \leq 1.49$ is weaker than the prior RIP-type conditions appeared in literature (Needell and Tropp 2009, Bahmani et al. 2013, Yuan et al. 2017). Finally, it is worthy to emphasize that, in Section 3.4, we will relax the RIP-type condition and obtain similar properties in sparse solution and computation.

3.2. Guarantees on Solution

The following theorem is one of the main results in this paper:

THEOREM 1. *Suppose Algorithm 1 returns $(\hat{\boldsymbol{\theta}}, \hat{\mathcal{A}})$, then $\hat{\mathcal{A}} = \mathcal{A}^*$ holds under Assumptions 1-2.*

Theorem 1 ensures SCOPE exactly recovers the true support set, which has been pursued for a long time in literature (Liu et al. 2014, Yuan et al. 2017, 2020, Zhou et al. 2021). Compared with the algorithms in the literature, the core advantage of SCOPE is that it guarantees to recover the true support set so long as the objective function enjoys certain assumptions. On the contrary, the success of the other algorithms requires tuning parameters such as the step size (Yuan et al. 2017, 2020) and the convergence criteria are properly set (Liu et al. 2014). Unfortunately, the tuning parameters may not be easily determined in practice. For instance, the suitable step size in Yuan et al. (2017, 2020) should be less than M_{2s}^{-1} albeit it is not too intensive to compute because we have to consider $\binom{2s}{p}$ subspaces with dimension $2s$. As we can see in Section 6, once the step size is incorrectly set, algorithms may fail to recover the true solution.

The tuning-free property of SCOPE comes from two aspects. First, it utilizes the splicing operation to find the support set that minimizes the objective function. As mentioned in Remark 2, the minimizer always exists without tuning any continuous parameter. In contrast, many iterative algorithms find the stable

solution of the support sets that are derived from the estimated parameters during iterations. Since the parameter estimation with gradient descent is sensitive to the choice of step size, selecting an adequate step size is crucial for these algorithms to correctly select the true support set (see, e.g., Yuan et al. (2017)). Second, SCOPE fully leverages the information of s . While iterative algorithms that shift the support size during iterations pay additional costs to find the true support set (e.g., Liu et al. (2014)).

Proof sketch for Theorem 1. Before proving Theorem 1, we present three crucial Lemmas. Among them, the first two Lemmas establish the lower and upper bounds for $\nabla_{\mathcal{A}}^2 f(\boldsymbol{\theta})$ and $\nabla_{\mathcal{A}} \nabla_{\mathcal{B}} f(\boldsymbol{\theta})$ where $\boldsymbol{\theta}$ is an arbitrary sparse parameter, and \mathcal{A}, \mathcal{B} are arbitrary support sets.

LEMMA 1. *If $f : \mathbb{R}^p \mapsto \mathbb{R}$ is twice differentiable and is m_k -RSC and M_k -RSS, then, for $\forall \mathcal{A} \subseteq [p], \mathbf{x} \in \mathbb{R}^p$ satisfying $|\mathcal{A} \cup \text{supp}(\mathbf{x})| \leq k$, we have: $m_k I_{|\mathcal{A}|} \preceq \nabla_{\mathcal{A}}^2 f(\mathbf{x}) \preceq M_k I_{|\mathcal{A}|}$.*

LEMMA 2. *If $f : \mathbb{R}^p \mapsto \mathbb{R}$ is m_k -RSS and M_k -RSC and has the second differentiation, then $\forall \mathcal{A}, \mathcal{B} \subseteq [p], \mathbf{x} \in \mathbb{R}^p$ satisfying $|\mathcal{A} \cup \mathcal{B} \cup \text{supp}(\mathbf{x})| \leq k$ and $\mathcal{A} \cap \mathcal{B} = \emptyset$, we have:*

$$\|\nabla_{\mathcal{A}} \nabla_{\mathcal{B}} f(\mathbf{x}) v\| \leq \frac{M_k - m_k}{2} \|v\| \quad \text{and} \quad w^\top \nabla_{\mathcal{A}} \nabla_{\mathcal{B}} f(\mathbf{x}) v \leq \frac{M_k - m_k}{2} \|w\| \|v\|,$$

$$\forall v \in \mathbb{R}^{|\mathcal{A}|}, w \in \mathbb{R}^{|\mathcal{B}|}.$$

Together with Taylor expansion at $\boldsymbol{\theta}^*$, the two Lemmas facilitate the control for $f(\boldsymbol{\theta}) - f(\boldsymbol{\theta}^*)$. These two Lemmas can be proven under Assumption 1.

Next, Lemma 3 shows that whenever we encounter a sparse solution whose support set is not identical to \mathcal{A}^* , then the objective function value at this sparse solution can be bounded. This bound is derived from the previous two Lemmas and Assumption 2. More interestingly, this lemma shows that, for the following sparse solution derived by one splicing operator, the value of the objective function at this new solution can be controlled by similar terms for bounding the previous sparse solution. Therefore, Lemma 3 enables the comparison of $f(\cdot)$ at the two sparse solutions.

LEMMA 3. *Let $\hat{\boldsymbol{\theta}}$ is any estimation in the splicing loop whose support set $\hat{\mathcal{A}}$ does not equal to \mathcal{A}^* , i.e., $\mathcal{I}_1 := \hat{\mathcal{I}} \cap \mathcal{A}^* \neq \emptyset$, and we define $\tilde{\boldsymbol{\theta}}$ as an estimation under a new support set $\tilde{\mathcal{A}}$ given by one splicing operation: $\tilde{\mathcal{A}} := (\text{supp}\{\hat{\boldsymbol{\theta}}\} \cup \mathcal{S}_{|\mathcal{I}_1|}^{\mathcal{I}}) \setminus \mathcal{S}_{|\mathcal{I}_1|}^{\mathcal{A}}$. Support Assumptions 1-2 hold, and let $m := m_{3s}$, $M := M_{3s}$, $v := \frac{M-m}{2}$, $c := \frac{0.35}{\sqrt{s}}(1.49m - M)$, then we have:*

$$f(\hat{\boldsymbol{\theta}}) - f(\boldsymbol{\theta}^*) \geq \left(\frac{m}{2} - \sqrt{2sc}\right) \|\boldsymbol{\theta}_{\mathcal{I}_1}^*\|^2, \quad (5)$$

$$|f(\tilde{\boldsymbol{\theta}}) - f(\boldsymbol{\theta}^*)| \leq \left[\frac{sc^2}{m} + \frac{sc^2 M}{2m^2} + \left(\frac{\sqrt{sc}v}{m} + \frac{\sqrt{sc}Mv}{m^2} + \sqrt{sc}\right)\Delta + \left(\frac{Mv^2}{2m^2} + \frac{M}{2}\right)\Delta^2 \right] \|\boldsymbol{\theta}_{\mathcal{I}_1}^*\|^2, \quad (6)$$

where Δ is a constant depends on m, M and s .

We prove Theorem 1 by showing that if $\hat{\mathcal{A}} \neq \mathcal{A}^*$, it would cause a contradiction. Notably, Lemma 3 allows us to analyze the loss at a support set $\tilde{\mathcal{A}}$ attained by one splicing operation upon $\hat{\mathcal{A}}$. By comparing the f under $\hat{\mathcal{A}}$ or $\tilde{\mathcal{A}}$, we find $\min_{\text{supp}\{\boldsymbol{\theta}\}=\hat{\mathcal{A}}} f(\boldsymbol{\theta}) > \min_{\text{supp}\{\boldsymbol{\theta}\}=\tilde{\mathcal{A}}} f(\boldsymbol{\theta})$ hold under Assumption 2. This implies $\hat{\mathcal{A}}$ should not be the support convergence point, which contradicts the fact that Algorithm 1 outputs $\hat{\mathcal{A}}$. Therefore, our primary supposition is incorrect, and $\hat{\mathcal{A}} = \mathcal{A}^*$ must hold.

Now, we present a direct result of Theorem 1 that reveals the property of the parameter estimation returned by Algorithm 1. Denote the oracle solution $\hat{\boldsymbol{\theta}}^*$ as $\hat{\boldsymbol{\theta}}^* := \arg \min_{\text{supp}\{\boldsymbol{\theta}\}=\mathcal{A}^*} f(\boldsymbol{\theta})$, then we have the following results.

COROLLARY 1. *Under Assumptions 1-2, $\hat{\boldsymbol{\theta}} = \hat{\boldsymbol{\theta}}^*$. Particularly, if $\|\nabla f(\boldsymbol{\theta}^*)\|_\infty = 0$, then $\hat{\boldsymbol{\theta}} = \boldsymbol{\theta}^*$.*

3.3. Convergence Analysis

This section mainly asserts the computational efficiency of Algorithm 1. We first show that Algorithm 1 has a linear convergence rate.

THEOREM 2. *Follow with Assumptions in Theorem 1, there exists a constant $\delta_1 > 1$ such that*

$$|f(\boldsymbol{\theta}^{t+1}) - f(\boldsymbol{\theta}^*)| \leq \delta_1^{-1} |f(\boldsymbol{\theta}^t) - f(\boldsymbol{\theta}^*)|, \quad (7)$$

when $\boldsymbol{\theta}^t$ is not the output of Algorithm 1.

Theorem 2 claims that, so long as the SCOPE algorithm has not converged, then the splicing operator would give a new solution that substantially decreases the objective function value. From this property, we can deduce SCOPE converges quickly. Though similar properties are achieved in literature (Bahmani et al. 2013, Yuan et al. 2017, 2020), it is remarkable that our result is obtained without tuning continuous parameters like Bahmani et al. (2013).

Proof sketch of Theorem 2. From Lemma 3, we can give the bounds of objective function values on the current solution $\boldsymbol{\theta}^t$ and the next solution $\boldsymbol{\theta}^{t+1}$. By the RIP-type condition implied by Assumption 2, we will show that the ratio of these two bounds is not more than a constant that is less than 1. Therefore, the algorithm converges linearly.

Our next theorem explicitly derives the lower bound for the number of iterations to recover \mathcal{A}^* .

THEOREM 3. *Suppose Assumptions in Theorem 1 hold, then there is a constant $\delta_2 > 0$ such that the number of splicing iterations needed for support recovery $\mathcal{A}^t = \mathcal{A}^*$ is lower bounded by*

$$t \geq \log_{\delta_1} \left\lceil \frac{|f(\boldsymbol{\theta}^0) - f(\boldsymbol{\theta}^*)|}{\delta_2 m_{3s} \vartheta^2} \right\rceil, \quad (8)$$

where $\lceil \cdot \rceil$ is the ceiling function, δ_1 is defined in Theorem 2, and $f(\boldsymbol{\theta}^0) := \min_{\text{supp}\{\boldsymbol{\theta}\}=\mathcal{A}^0} f(\boldsymbol{\theta})$ in which \mathcal{A}^0 is an arbitrary s -cardinality subset of $[p]$.

Theorem 3 guarantees the splicing iteration makes the algorithm identify the true active set within a few iterations. It also indicates the quality of the initial activation set \mathcal{A}^0 , and the size of the minimum signal affects the minimum number of iterations. Specifically, SCOPE requires fewer splicing iterations to converge when a good initial active set is available, or the minimum signal is large.

3.4. Properties without RIP-type Conditions

As discussed in Section 3.1, Assumption 2 encompasses a RIP-type condition, which may be restrictive in practical scenarios. However, the following theorems show that appropriately relaxing sparsity levels enables the SCOPE to accurately estimate sparse solutions without assuming the RIP-type condition.

To establish the theorems, we first provide the mathematical characterization of the conditions required in this section. In this part, we denote $s^* := |\mathcal{A}^*|$ and let $s := |\hat{\mathcal{A}}|$. The two conditions are given below.

ASSUMPTION 3. $f(\cdot)$ is m_{s+s^*} -RSC and M_{s+s^*} -RSS.

ASSUMPTION 4. $\|\nabla f(\boldsymbol{\theta}^*)\|_\infty < \frac{m_{s+s^*}}{2\sqrt{s+s^*}}\vartheta$ where m_{s+s^*} is defined in Assumption 3.

Assumption 3 characterizes the relaxing sparsity levels mentioned earlier, requiring $f(\boldsymbol{\theta})$ to exhibit strong convexity and strong smoothness on any $(s + s^*)$ -dimensional subspace. The second assumption relates to the systematic noise, ensuring that the noise is controlled by the minimal magnitude of the sparse signal and decays to zero with a rate of $O(s^{-\frac{1}{2}})$. This rate aligns with Assumption 2 and matches the rate in previous studies (Jain et al. 2014, Yuan et al. 2017). More importantly, the constant involved in Assumption 4 is only proportional to the m_{s+s^*} and is independent to the restricted condition number $\frac{M_{s+s^*}}{m_{s+s^*}}$ in Assumption 2. Consequently, this assumption essentially frees from RIP-type conditions.

We now present the guarantee for the solution when sparsity levels are relaxed.

THEOREM 4. Suppose Assumptions 3 and 4 hold when setting $s > (1 + 2\frac{M_{s+s^*}^2}{m_{s+s^*}^2})s^*$. Then, $(\hat{\boldsymbol{\theta}}, \hat{\mathcal{A}})$ satisfies (i) $\hat{\mathcal{A}} \supseteq \mathcal{A}^*$ and (ii) $\text{supp}(\mathcal{H}_{s^*}(\hat{\boldsymbol{\theta}})) = \mathcal{A}^*$.

From Theorem 4, the SCOPE gives an estimated support set that includes the true support set. Even more interestingly, (ii) reveals the top s^* coordinates (in the sense of magnitude) in $\hat{\boldsymbol{\theta}}$ are exactly the true support set. It is worth noting that while the sparsity level shall increase linearly with respect to the restricted condition number, the rate of increase is slower compared to Jain et al. (2014) and Yuan et al. (2017). This advantage arises from the fact that, in each splicing iteration, Algorithm 1 effectively utilizes the objective value to identify an appropriate splicing set. To prove Theorem 4, we reuse the results of Lemmas 1 and 2, and further, we develop Lemma 4 that bounds the gap of objective between the current solution and the spliced set.

LEMMA 4. Let $\hat{\boldsymbol{\theta}}$ be the s -sparse solution under a support set $\hat{\mathcal{A}}$. Denote $\rho_0 := 0, \rho_j := \frac{\max\{|\hat{\boldsymbol{\theta}}_i| : i \in \mathcal{S}_{\hat{\mathcal{A}}}^{(j)}\}}{\min\{|\nabla_i f(\hat{\boldsymbol{\theta}})| : i \in \mathcal{S}_{\hat{\mathcal{A}}}^{(j)}\}}$ (for $j \in [s^*]$), and $\rho_{s^*+1} = +\infty$. Under Assumption 3, for $\forall \varepsilon > 0$, there exists $k \in$

$\{0, \dots, s^*\}$ satisfying $\frac{1}{M_{s+s^*} + \varepsilon} \in [\rho_k, \rho_{k+1}]$ such that, given the support set $\tilde{\mathcal{A}}^k := (\hat{\mathcal{A}} \setminus \mathcal{S}_{\hat{\mathcal{A}}}^{(k)}) \cup \mathcal{S}_{\mathcal{I}}^{(k)}$, $\tilde{\boldsymbol{\theta}}^{(k)} := \arg \min_{\text{supp}\{\boldsymbol{\theta}\}=\tilde{\mathcal{A}}^k} f(\boldsymbol{\theta})$ satisfies

$$f(\tilde{\boldsymbol{\theta}}^{(k)}) - f(\hat{\boldsymbol{\theta}}) \leq \frac{-\varepsilon}{2(M_{s+s^*} + \varepsilon)^2} \left\| \nabla f(\hat{\boldsymbol{\theta}})_{\mathcal{S}_{\mathcal{I}}^{(k)}} \right\|^2. \quad (9)$$

Our next Theorem demonstrates that even without imposing RIP-type conditions, Algorithm 1 still exhibits a linear convergence rate when the sparsity level is relaxed.

THEOREM 5. *Suppose Assumption 3 holds when setting $s > 2(1 + 2\frac{M_{s+s^*}^2}{m_{s+s^*}^2})s^*$ in Algorithm 1, then*

$$f(\boldsymbol{\theta}^{t+1}) - f(\boldsymbol{\theta}^*) \leq (1 - \delta_4) (f(\boldsymbol{\theta}^t) - f(\boldsymbol{\theta}^*)),$$

when $f(\boldsymbol{\theta}^t) \geq f(\boldsymbol{\theta}^*)$ and $\boldsymbol{\theta}^t$ is not the solution of Algorithm 1, where $\delta_4 = \frac{m_{s+s^*}}{4M_{s+s^*}} \left(1 - \frac{4s^*}{s-2s^*} \frac{M_{s+s^*}^2}{m_{s+s^*}^2} \right) \in (0, \frac{m_{s+s^*}}{4M_{s+s^*}})$.

In comparison to Theorem 2, Theorem 5 does not require the constraint on $\|\nabla f(\boldsymbol{\theta}^*)\|_\infty$. This is because Assumption 3 imposes an RSC and RSS assumption on higher dimensional subspaces, which simplifies the analysis for the deduction of the objective value after each splicing iteration.

With the linear convergence rate established in Theorem 5, we can derive the number of splicing iterations for including \mathcal{A}^* when the sparsity level is relaxed.

THEOREM 6. *Under the same conditions and notations in Theorem 5 and if Assumption 4 also holds, we have $\mathcal{A}^t \supseteq \mathcal{A}^*$ when the number of splicing iterations t satisfies*

$$t \geq \log_{(1-\delta_4)^{-1}} \left\lceil \frac{\max\{f(\boldsymbol{\theta}^0) - f(\boldsymbol{\theta}^*), 0\}}{(\frac{1}{2} - \delta_5)m_{s+s^*}\vartheta^2} \right\rceil,$$

where δ_5 is a constant.

4. Proof of Main Theoretical Results

We prove our main theoretical results in this section.

4.1. Proof under RIP-type Conditions

Proof of Lemma 3. Define $\mathcal{I}_2 = \hat{\mathcal{I}} \cap \mathcal{I}^*$, $\mathcal{A}_1 = \hat{\mathcal{A}} \cap \mathcal{A}^*$, $\mathcal{A}_2 = \hat{\mathcal{A}} \cap \mathcal{I}^*$. For ease notations, we denote $\mathbf{d}^* = \nabla f(\boldsymbol{\theta}^*)$, $\hat{\mathbf{d}} = \nabla f(\hat{\boldsymbol{\theta}})$, and $\mathcal{S}_1 = \mathcal{S}_{\hat{\mathcal{A}}}^{(|\mathcal{I}_1|)}$, where $|\mathcal{I}_1|$ means the cardinality of \mathcal{I}_1 . Also, denote $\mathcal{A}_{11} = \mathcal{A}_1 \cap (\mathcal{S}_1)^c$, $\mathcal{A}_{12} = \mathcal{A}_1 \cap \mathcal{S}_1$, $\mathcal{A}_{21} = \mathcal{A}_2 \cap (\mathcal{S}_1)^c$, $\mathcal{A}_{22} = \mathcal{A}_2 \cap \mathcal{S}_1$. Then $\mathcal{S}_1 = \mathcal{A}_{12} \cup \mathcal{A}_{22}$. Since $|\mathcal{A}_{12}| + |\mathcal{A}_{22}| = |\mathcal{I}_1| = |\mathcal{A}^*| - |\mathcal{A}_1| \leq |\hat{\mathcal{A}}| - |\mathcal{A}_1| = |\mathcal{A}_2| = |\mathcal{A}_{21}| + |\mathcal{A}_{22}|$, we have $|\mathcal{A}_{12}| \leq |\mathcal{A}_{21}|$.

By definition of \mathcal{S}_1 , we have

$$\hat{\boldsymbol{\theta}}_j^2 \leq \hat{\boldsymbol{\theta}}_i^2, \quad \forall j \in \mathcal{A}_{12}, i \in \mathcal{A}_{21}.$$

Thus,

$$\|\hat{\boldsymbol{\theta}}_{\mathcal{A}_{12}}\| \leq \|\hat{\boldsymbol{\theta}}_{\mathcal{A}_{21}}\|. \quad (10)$$

Since $\hat{\boldsymbol{\theta}}$ minimizes $f(\boldsymbol{\theta})$ given active set $\hat{\mathcal{A}}$, $0 = \nabla_{\hat{\mathcal{A}}} f(\hat{\boldsymbol{\theta}}) = \nabla_{\hat{\mathcal{A}}} f(\boldsymbol{\theta}^*) + \nabla_{\hat{\mathcal{A}}}^2 f(\bar{\boldsymbol{\theta}})(\hat{\boldsymbol{\theta}}_{\hat{\mathcal{A}}} - \boldsymbol{\theta}_{\hat{\mathcal{A}}}^*) + \nabla_{\hat{\mathcal{A}}} \nabla_{\mathcal{I}_1} f(\bar{\boldsymbol{\theta}})(-\boldsymbol{\theta}_{\mathcal{I}_1}^*)$, where $\bar{\boldsymbol{\theta}} = t\hat{\boldsymbol{\theta}} + (1-t)\boldsymbol{\theta}^*$, $0 \leq t \leq 1$. By Lemma 1 and Lemma 2, we have

$$\begin{aligned} \|\hat{\boldsymbol{\theta}}_{\hat{\mathcal{A}}} - \boldsymbol{\theta}_{\hat{\mathcal{A}}}^*\| &\leq \|[\nabla_{\hat{\mathcal{A}}}^2 f(\bar{\boldsymbol{\theta}})]^{-1} \mathbf{d}_{\hat{\mathcal{A}}}^*\| + \|[\nabla_{\hat{\mathcal{A}}}^2 f(\bar{\boldsymbol{\theta}})]^{-1} \cdot \nabla_{\hat{\mathcal{A}}} \nabla_{\mathcal{I}_1} f(\bar{\boldsymbol{\theta}}) \cdot \boldsymbol{\theta}_{\mathcal{I}_1}^*\| \\ &\leq m^{-1} \|\mathbf{d}_{\hat{\mathcal{A}}}^*\| + m^{-1} v \|\boldsymbol{\theta}_{\mathcal{I}_1}^*\|. \end{aligned} \quad (11)$$

Thus, the loss function at the point $\hat{\boldsymbol{\theta}}$ satisfies:

$$\begin{aligned} f(\hat{\boldsymbol{\theta}}) - f(\boldsymbol{\theta}^*) &\geq (\hat{\boldsymbol{\theta}} - \boldsymbol{\theta}^*)^\top \mathbf{d}^* + \frac{m}{2} \|\hat{\boldsymbol{\theta}} - \boldsymbol{\theta}^*\|^2 \\ &\geq \frac{m}{2} \|\hat{\boldsymbol{\theta}} - \boldsymbol{\theta}^*\|^2 - \|\mathbf{d}_{\mathcal{I}_2^c}^*\| \|\hat{\boldsymbol{\theta}} - \boldsymbol{\theta}^*\| \\ &= \frac{m}{2} \left(\|\hat{\boldsymbol{\theta}} - \boldsymbol{\theta}^*\| - \frac{1}{m} \|\mathbf{d}_{\mathcal{I}_2^c}^*\| \right)^2 - \frac{1}{2m} \|\mathbf{d}_{\mathcal{I}_2^c}^*\|^2. \end{aligned}$$

$$\text{By } \|\hat{\boldsymbol{\theta}} - \boldsymbol{\theta}^*\| \geq \|\boldsymbol{\theta}_{\mathcal{I}_1}^*\| \geq \vartheta \geq \frac{\sqrt{s}}{0.35(1.49 - \frac{M}{m})m} \|\mathbf{d}^*\|_\infty \geq \frac{\sqrt{2s}}{m} \|\mathbf{d}^*\|_\infty \geq \frac{1}{m} \|\mathbf{d}_{\mathcal{I}_2^c}^*\|,$$

$$f(\hat{\boldsymbol{\theta}}) - f(\boldsymbol{\theta}^*) \geq \frac{m}{2} \|\boldsymbol{\theta}_{\mathcal{I}_1}^*\|^2 - \|\mathbf{d}_{\mathcal{I}_2^c}^*\| \|\boldsymbol{\theta}_{\mathcal{I}_1}^*\| \geq \left(\frac{m}{2} - \sqrt{2sc} \right) \|\boldsymbol{\theta}_{\mathcal{I}_1}^*\|^2. \quad (12)$$

Next, we derive an upper bound for $\|\boldsymbol{\theta}_{\mathcal{A}_{12}}^*\|$ and $\|\boldsymbol{\theta}_{\mathcal{I}_{12}}^*\|$ (defined below) to bound the loss function at the point $\tilde{\boldsymbol{\theta}}$. Notably, from inequality (11), it can be derived that

$$\begin{aligned} \|\hat{\boldsymbol{\theta}}_{\mathcal{A}_{12}}\| &\geq \|\boldsymbol{\theta}_{\mathcal{A}_{12}}^*\| - \|\hat{\boldsymbol{\theta}}_{\hat{\mathcal{A}}} - \boldsymbol{\theta}_{\hat{\mathcal{A}}}^*\| \geq \|\boldsymbol{\theta}_{\mathcal{A}_{12}}^*\| - \frac{1}{m} \|\mathbf{d}_{\hat{\mathcal{A}}}^*\| - \frac{v}{m} \|\boldsymbol{\theta}_{\mathcal{I}_1}^*\|, \\ \|\hat{\boldsymbol{\theta}}_{\mathcal{A}_{21}}\| &\leq \|\boldsymbol{\theta}_{\mathcal{A}_{21}}^*\| + \|\hat{\boldsymbol{\theta}}_{\hat{\mathcal{A}}} - \boldsymbol{\theta}_{\hat{\mathcal{A}}}^*\| \leq \frac{1}{m} \|\mathbf{d}_{\hat{\mathcal{A}}}^*\| + \frac{v}{m} \|\boldsymbol{\theta}_{\mathcal{I}_1}^*\|. \end{aligned}$$

Furthermore, by (10), we have

$$\begin{aligned} \|\boldsymbol{\theta}_{\mathcal{A}_{12}}^*\| &\leq 2 \left(\frac{1}{m} \|\mathbf{d}_{\hat{\mathcal{A}}}^*\| + \frac{v}{m} \|\boldsymbol{\theta}_{\mathcal{I}_1}^*\| \right) \\ &\leq \frac{2}{m} \left(c \sqrt{\frac{s}{|\mathcal{I}_1|}} + v \right) \|\boldsymbol{\theta}_{\mathcal{I}_1}^*\| \\ &\leq 2 \left(\frac{\sqrt{sc}}{m} + \frac{v}{m} \right) \|\boldsymbol{\theta}_{\mathcal{I}_1}^*\|, \end{aligned} \quad (13)$$

where the second inequality follows from Assumption 2.

On the other hand, denote $\mathcal{S}_2 = \mathcal{S}_{\mathcal{I}}^{(|\mathcal{I}_1|)}$ and $\mathcal{I}_{11} = \mathcal{I}_1 \cap \mathcal{S}_2$, $\mathcal{I}_{12} = \mathcal{I}_1 \cap (\mathcal{S}_2)^c$, $\mathcal{I}_{21} = \mathcal{I}_2 \cap \mathcal{S}_2$, $\mathcal{I}_{22} = \mathcal{I}_2 \cap (\mathcal{S}_2)^c$.

Since $|\mathcal{I}_{11}| + |\mathcal{I}_{21}| = |\mathcal{S}_2| = |\mathcal{I}_1| = |\mathcal{I}_{11}| + |\mathcal{I}_{12}|$, we have $|\mathcal{I}_{12}| = |\mathcal{I}_{21}|$. By definition of \mathcal{S}_2 , we have

$$\hat{\mathbf{d}}_i^2 \leq \hat{\mathbf{d}}_j^2, \quad \forall i \in \mathcal{I}_{12}, j \in \mathcal{I}_{21}.$$

Thus,

$$\|\hat{\mathbf{d}}_{\mathcal{I}_{12}}\| \leq \|\hat{\mathbf{d}}_{\mathcal{I}_{21}}\|. \quad (14)$$

Note that,

$$\hat{\mathbf{d}}_{\hat{\mathcal{I}}} = \nabla_{\hat{\mathcal{I}}} f(\hat{\boldsymbol{\theta}}) = \nabla_{\hat{\mathcal{I}}} f(\boldsymbol{\theta}^*) + \nabla_{\hat{\mathcal{A}}} \nabla_{\hat{\mathcal{I}}} f(\bar{\boldsymbol{\theta}})(\hat{\boldsymbol{\theta}}_{\hat{\mathcal{A}}} - \boldsymbol{\theta}_{\hat{\mathcal{A}}}^*) + \nabla_{\mathcal{I}_1} \nabla_{\hat{\mathcal{I}}} f(\bar{\boldsymbol{\theta}})(-\boldsymbol{\theta}_{\mathcal{I}_1}^*), \quad (15)$$

where $\bar{\boldsymbol{\theta}} = t\hat{\boldsymbol{\theta}} + (1-t)\boldsymbol{\theta}^*$, $0 \leq t \leq 1$. Then, by (15),

$$\begin{aligned} \|\hat{\mathbf{d}}_{\mathcal{I}_{12}}\| &\geq -\|\nabla_{\mathcal{I}_{12}} f(\boldsymbol{\theta}^*)\| - \|\nabla_{\hat{\mathcal{A}}} \nabla_{\mathcal{I}_{12}} f(\bar{\boldsymbol{\theta}})(\hat{\boldsymbol{\theta}}_{\hat{\mathcal{A}}} - \boldsymbol{\theta}_{\hat{\mathcal{A}}}^*)\| + \|\nabla_{\mathcal{I}_{12}}^2 f(\bar{\boldsymbol{\theta}})\boldsymbol{\theta}_{\mathcal{I}_{12}}^*\| - \|\nabla_{\mathcal{I}_{11}} \nabla_{\mathcal{I}_{12}} f(\bar{\boldsymbol{\theta}})\boldsymbol{\theta}_{\mathcal{I}_1}^*\| \\ &\geq -\|\mathbf{d}_{\mathcal{I}_{12}}^*\| - v\|\hat{\boldsymbol{\theta}}_{\hat{\mathcal{A}}} - \boldsymbol{\theta}_{\hat{\mathcal{A}}}^*\| + m\|\boldsymbol{\theta}_{\mathcal{I}_{12}}^*\| - v\|\boldsymbol{\theta}_{\mathcal{I}_1}^*\| \\ &\geq m\|\boldsymbol{\theta}_{\mathcal{I}_{12}}^*\| - v\|\boldsymbol{\theta}_{\mathcal{I}_1}^*\| - \|\mathbf{d}_{\mathcal{I}_{12}}^*\| - \frac{v}{m}\|\mathbf{d}_{\hat{\mathcal{A}}}^*\| - \frac{v^2}{m}\|\boldsymbol{\theta}_{\mathcal{I}_1}^*\|, \\ \|\hat{\mathbf{d}}_{\mathcal{I}_{21}}\| &\leq \|\nabla_{\mathcal{I}_{21}} f(\boldsymbol{\theta}^*)\| + \|\nabla_{\hat{\mathcal{A}}} \nabla_{\mathcal{I}_{21}} f(\bar{\boldsymbol{\theta}})(\hat{\boldsymbol{\theta}}_{\hat{\mathcal{A}}} - \boldsymbol{\theta}_{\hat{\mathcal{A}}}^*)\| + \|\nabla_{\mathcal{I}_1} \nabla_{\mathcal{I}_{21}} f(\bar{\boldsymbol{\theta}})\boldsymbol{\theta}_{\mathcal{I}_1}^*\| \\ &\leq \|\mathbf{d}_{\mathcal{I}_{21}}^*\| + v\|\hat{\boldsymbol{\theta}}_{\hat{\mathcal{A}}} - \boldsymbol{\theta}_{\hat{\mathcal{A}}}^*\| + v\|\boldsymbol{\theta}_{\mathcal{I}_1}^*\| \\ &\leq \|\mathbf{d}_{\mathcal{I}_{21}}^*\| + \frac{v}{m}\|\mathbf{d}_{\hat{\mathcal{A}}}^*\| + \frac{v^2}{m}\|\boldsymbol{\theta}_{\mathcal{I}_1}^*\| + v\|\boldsymbol{\theta}_{\mathcal{I}_1}^*\|. \end{aligned}$$

In conjunction with (14), we have

$$\|\mathbf{d}_{\mathcal{I}_{21}}^*\| + \frac{v}{m}\|\mathbf{d}_{\hat{\mathcal{A}}}^*\| + \left(\frac{v^2}{m} + v\right)\|\boldsymbol{\theta}_{\mathcal{I}_1}^*\| \geq m\|\boldsymbol{\theta}_{\mathcal{I}_{12}}^*\| - v\|\boldsymbol{\theta}_{\mathcal{I}_1}^*\| - \|\mathbf{d}_{\mathcal{I}_{12}}^*\| - \frac{v}{m}\|\mathbf{d}_{\hat{\mathcal{A}}}^*\| - \frac{v^2}{m}\|\boldsymbol{\theta}_{\mathcal{I}_1}^*\|.$$

Thus, we have

$$\begin{aligned} \frac{\|\boldsymbol{\theta}_{\mathcal{I}_{12}}^*\|}{\|\boldsymbol{\theta}_{\mathcal{I}_1}^*\|} &\leq \frac{1}{m\|\boldsymbol{\theta}_{\mathcal{I}_1}^*\|} \left[\|\mathbf{d}_{\mathcal{I}_{21}}^*\| + \|\mathbf{d}_{\mathcal{I}_{12}}^*\| + 2\frac{v}{m}\|\mathbf{d}_{\hat{\mathcal{A}}}^*\| + 2\left(\frac{v^2}{m} + v\right)\|\boldsymbol{\theta}_{\mathcal{I}_1}^*\| \right] \\ &\leq \frac{c}{\sqrt{|\mathcal{I}_1|}m} \left(\sqrt{|\mathcal{I}_{21}|} + \sqrt{|\mathcal{I}_{12}|} + \frac{2v}{m}\sqrt{s} \right) + 2\left(\frac{v^2}{m^2} + \frac{v}{m}\right) \\ &\leq 2\left(\frac{c}{m}\sqrt{\frac{|\mathcal{I}_{12}|}{|\mathcal{I}_1|}} + \frac{\sqrt{scv}}{m^2\sqrt{|\mathcal{I}_1|}} + \frac{v^2}{m^2} + \frac{v}{m}\right) \\ &\leq 2\left(\frac{\sqrt{sc}}{m} + \frac{\sqrt{scv}}{m^2} + \frac{v^2}{m^2} + \frac{v}{m}\right). \end{aligned}$$

Consider the new active set $\tilde{\mathcal{A}} = (\hat{\mathcal{A}} \setminus \mathcal{S}_1) \cup \mathcal{S}_2$ and inactive set $\tilde{\mathcal{I}} = (\tilde{\mathcal{A}})^c$. Similar to \mathcal{I}_1 , define $\tilde{\mathcal{I}}_1 = \tilde{\mathcal{I}} \cap \mathcal{A}^*$.

Since $\bar{\boldsymbol{\theta}} = \arg \min_{\boldsymbol{\theta}_{\tilde{\mathcal{I}}=0}} f(\boldsymbol{\theta})$, similar to (11), we have

$$\|\tilde{\boldsymbol{\theta}}_{\tilde{\mathcal{A}}} - \boldsymbol{\theta}_{\tilde{\mathcal{A}}}^*\| \leq m^{-1}\|\mathbf{d}_{\tilde{\mathcal{A}}}^*\| + \frac{v}{m}\|\boldsymbol{\theta}_{\tilde{\mathcal{I}}_1}^*\|.$$

Notice that $\tilde{\mathcal{I}}_1 = \mathcal{I}_{12} \cup \mathcal{A}_{12}$, the gap between the loss function at point $\tilde{\boldsymbol{\theta}}$ and $f(\boldsymbol{\theta}^*)$ can be expanded as:

$$\begin{aligned}
|f(\tilde{\boldsymbol{\theta}}) - f(\boldsymbol{\theta}^*)| &\leq |\nabla_{\tilde{\mathcal{A}}} f(\boldsymbol{\theta}^*)^\top (\tilde{\boldsymbol{\theta}}_{\tilde{\mathcal{A}}} - \boldsymbol{\theta}_{\tilde{\mathcal{A}}}^*)| + |\nabla_{\tilde{\mathcal{I}}_1} f(\boldsymbol{\theta}^*)^\top (-\boldsymbol{\theta}_{\tilde{\mathcal{I}}_1}^*)| + \frac{M}{2} \|\tilde{\boldsymbol{\theta}} - \boldsymbol{\theta}^*\|^2 \\
&\leq \|\mathbf{d}_{\tilde{\mathcal{A}}}^*\| \|\tilde{\boldsymbol{\theta}}_{\tilde{\mathcal{A}}} - \boldsymbol{\theta}_{\tilde{\mathcal{A}}}^*\| + \|\mathbf{d}_{\tilde{\mathcal{I}}_1}^*\| \|\boldsymbol{\theta}_{\tilde{\mathcal{I}}_1}^*\| + \frac{M}{2} \|\tilde{\boldsymbol{\theta}}_{\tilde{\mathcal{A}}} - \boldsymbol{\theta}_{\tilde{\mathcal{A}}}^*\|^2 + \frac{M}{2} \|\boldsymbol{\theta}_{\tilde{\mathcal{I}}_1}^*\|^2 \\
&\leq m^{-1} \|\mathbf{d}_{\tilde{\mathcal{A}}}^*\|^2 + \frac{v}{m} \|\mathbf{d}_{\mathcal{A}}^*\| \|\boldsymbol{\theta}_{\mathcal{I}_{12} \cup \mathcal{A}_{12}}^*\| + \|\mathbf{d}_{\tilde{\mathcal{I}}_1}^*\| \|\boldsymbol{\theta}_{\mathcal{I}_{12} \cup \mathcal{A}_{12}}^*\| + \frac{M}{2m^2} \|\mathbf{d}_{\tilde{\mathcal{A}}}^*\|^2 \\
&\quad + \frac{Mv}{m^2} \|\mathbf{d}_{\tilde{\mathcal{A}}}^*\| \|\boldsymbol{\theta}_{\mathcal{I}_{12} \cup \mathcal{A}_{12}}^*\| + \left(\frac{Mv^2}{2m^2} + \frac{M}{2}\right) \|\boldsymbol{\theta}_{\mathcal{I}_{12} \cup \mathcal{A}_{12}}^*\|^2 \\
&\leq \left(\frac{1}{m} + \frac{M}{2m^2}\right) \frac{sc^2}{|\mathcal{I}_1|} \|\boldsymbol{\theta}_{\mathcal{I}_1}^*\|^2 + c \left[\left(\frac{v}{m} + \frac{Mv}{m^2}\right) \sqrt{\frac{s}{|\mathcal{I}_1|}} + \sqrt{\frac{|\tilde{\mathcal{I}}_1|}{|\mathcal{I}_1|}} \right] \frac{\|\boldsymbol{\theta}_{\mathcal{I}_{12} \cup \mathcal{A}_{12}}^*\|}{\|\boldsymbol{\theta}_{\mathcal{I}_1}^*\|} \|\boldsymbol{\theta}_{\mathcal{I}_1}^*\|^2 \\
&\quad + \left(\frac{Mv^2}{2m^2} + \frac{M}{2}\right) \frac{\|\boldsymbol{\theta}_{\mathcal{I}_{12} \cup \mathcal{A}_{12}}^*\|^2}{\|\boldsymbol{\theta}_{\mathcal{I}_1}^*\|^2} \|\boldsymbol{\theta}_{\mathcal{I}_1}^*\|^2 \\
&\leq \left[\frac{sc^2}{m} + \frac{sc^2 M}{2m^2} + \left(\frac{\sqrt{scv}}{m} + \frac{\sqrt{sc} Mv}{m^2} + \sqrt{sc}\right) \Delta + \left(\frac{Mv^2}{2m^2} + \frac{M}{2}\right) \Delta^2 \right] \|\boldsymbol{\theta}_{\mathcal{I}_1}^*\|^2,
\end{aligned} \tag{16}$$

where $\Delta = 2\sqrt{\left(\frac{\sqrt{sc}}{m} + \frac{v}{m}\right)^2 + \left(\frac{\sqrt{sc}}{m} + \frac{\sqrt{scv}}{m^2} + \frac{v^2}{m^2} + \frac{v}{m}\right)^2}$. This encloses the proof of Lemma 3.

Proof of Theorem 1. Suppose $\hat{\mathcal{A}} \neq \mathcal{A}^*$, then according to inequalities (5) and (6) in Lemma 3, we have:

$$\begin{aligned}
\frac{f(\hat{\boldsymbol{\theta}}) - f(\tilde{\boldsymbol{\theta}})}{m \|\boldsymbol{\theta}_{\mathcal{I}_1}^*\|^2} &\geq \frac{1}{2} - \sqrt{2} \frac{\sqrt{sc}}{m} - \left(\frac{\sqrt{sc}}{m}\right)^2 - \frac{1}{2} \left(\frac{\sqrt{sc}}{m}\right)^2 \frac{M}{m} \\
&\quad - \frac{\sqrt{sc}}{m} \left(\frac{v}{m} + \frac{M}{m} \frac{v}{m} + 1\right) \Delta - \left(\frac{1}{2} \frac{M}{m} \left(\frac{v}{m}\right)^2 + \frac{1}{2} \frac{M}{m}\right) \Delta^2.
\end{aligned}$$

Denote $x = \frac{M}{m}$, then $\frac{v}{m} = \frac{x-1}{2}$, and $\frac{\sqrt{sc}}{m} = 0.35(1.49 - x)$, we have

$$f(\hat{\boldsymbol{\theta}}) - f(\tilde{\boldsymbol{\theta}}) \geq m \|\boldsymbol{\theta}_{\mathcal{I}_1}^*\|^2 \varepsilon\left(\frac{M}{m}\right),$$

where $\varepsilon(x) = \frac{1}{2} - \sqrt{2}(0.5215 - 0.35x) - (0.5215 - 0.35x)^2 - \frac{1}{2}x(0.5215 - 0.35x)^2 - \frac{1}{2}(0.5215 - 0.35x)(x^2 + 1)\Delta(x) - \frac{1}{8}x(x^2 - 2x + 5)\Delta(x)^2$, and $\Delta(x) = (0.15x + 0.0215)\sqrt{x^2 + 2x + 5}$.

By Assumption 2, we know $x \in [1, 1.49]$, and in this interval, it's easy to prove $\varepsilon(x) > 0.0125$ which leads to a contradiction, thus $\hat{\mathcal{A}} = \mathcal{A}^*$.

Proof of Theorem 2. We reuse the notions such as $m, M, v, x, \Delta(x)$ in the proof of Theorem 1. Let $\Delta = 2\sqrt{\left(\frac{\sqrt{sc}}{m} + \frac{v}{m}\right)^2 + \left(\frac{\sqrt{sc}}{m} + \frac{\sqrt{scv}}{m^2} + \frac{v^2}{m^2} + \frac{v}{m}\right)^2}$, then by Assumption 2, we have:

$$\begin{aligned}
\frac{|f(\boldsymbol{\theta}^{t+1}) - f(\boldsymbol{\theta}^*)|}{|f(\boldsymbol{\theta}^t) - f(\boldsymbol{\theta}^*)|} &\leq \frac{\frac{sc^2}{m} + \frac{sc^2 M}{2m^2} + \left(\frac{\sqrt{scv}}{m} + \frac{\sqrt{sc} Mv}{m^2} + \sqrt{sc}\right) \Delta + \left(\frac{Mv^2}{2m^2} + \frac{M}{2}\right) \Delta^2}{\frac{m}{2} - \sqrt{2sc}} \\
&\leq \left[\frac{1}{2} - \sqrt{2}(0.5215 - 0.35x)\right]^{-1} [(0.5215 - 0.35x)^2 \\
&\quad + \frac{1}{2}x(0.5215 - 0.35x)^2 + \frac{1}{2}(0.5215 - 0.35x)(x^2 + 1)\Delta(x) \\
&\quad + \frac{1}{8}x(x^2 - 2x + 5)\Delta(x)^2],
\end{aligned} \tag{17}$$

where the first inequality follows from inequalities (5) and (6) given by Lemma 3, and the second inequality comes from $x = \frac{M}{m}$, $\frac{v}{m} = \frac{x-1}{2}$ and $\frac{\sqrt{sc}}{m} = 0.35(1.49 - x)$.

Furthermore, from Assumption 2, we know $x \in [1, 1.49]$. It is easy to prove that the univariate function in the right-hand side of (17), denoted by $\delta(x)$, satisfies $\delta_1^{-1} := \max_{x \in [1, 1.49]} \delta(x) < 0.968$. Consequently, we have:

$$|f(\boldsymbol{\theta}^{t+1}) - f(\boldsymbol{\theta}^*)| \leq \delta_1^{-1} |f(\boldsymbol{\theta}^t) - f(\boldsymbol{\theta}^*)|,$$

which completes the proof.

Proof of Theorem 3. Here, the notations $m, M, v, x, \Delta(x)$ adopt from the proof of Theorem 1. For each $\boldsymbol{\theta}^t$ whose support set is not equal to \mathcal{A}^* , we have

$$f(\boldsymbol{\theta}^t) - f(\boldsymbol{\theta}^*) \geq \left(\frac{1}{2} - \sqrt{2}(0.5215 - 0.35x)\right)m\vartheta > 0.2574m\vartheta^2,$$

where the first inequality comes from the inequality (5) in Lemma 3. So, there is a constant $\delta_2 > 0$ such that

$$f(\boldsymbol{\theta}^t) - f(\boldsymbol{\theta}^*) > \delta_2 m \vartheta^2. \quad (18)$$

On the other hand, if $t > \log_{\delta_1} \left[\frac{|f(\boldsymbol{\theta}^0) - f(\boldsymbol{\theta}^*)|}{\delta_2 m \vartheta^2} \right]$, Theorem 2 asserts that

$$|f(\boldsymbol{\theta}^t) - f(\boldsymbol{\theta}^*)| \leq \delta_1^{-t} |f(\boldsymbol{\theta}^0) - f(\boldsymbol{\theta}^*)| < \delta_2 m \vartheta^2, \quad (19)$$

where the first inequality raises from (7). However, (18) contradicts to (19), implying $\mathcal{A}^t = \mathcal{A}^*$ must hold when $t > \log_{\delta_1} \left[\frac{|f(\boldsymbol{\theta}^0) - f(\boldsymbol{\theta}^*)|}{\delta_2 m \vartheta^2} \right]$.

4.2. Proof without RIP-type Conditions

Proof of Lemma 4. We reuse the notions in the proof of Lemma 3 (e.g., we denote $M = M_{s+s^*}$). It is directly to see that $\rho_0 \leq \rho_1 \leq \dots \leq \rho_{s^*} \leq \rho_{s^*+1}$. When $M^{-1} \leq \rho_1$, selecting $k = 0$ makes the conclusion trivially hold. Consider the case that $M^{-1} \geq \rho_1$, we construct an auxiliary s -sparse vector $\bar{\boldsymbol{\theta}} \in \mathbb{R}^p$:

$$\bar{\boldsymbol{\theta}} = \begin{cases} \hat{\boldsymbol{\theta}}_i, & \text{if } i \in \hat{\mathcal{A}} \setminus \mathcal{S}_{\mathcal{A}}^{(k)} \\ \frac{-1}{M+\epsilon} \hat{\boldsymbol{d}}_i, & \text{if } i \in \mathcal{S}_{\mathcal{I}}^{(k)} \\ 0, & \text{if } i \in \mathcal{S}_{\mathcal{A}}^{(k)} \cup (\hat{\mathcal{I}} \setminus \mathcal{S}_{\mathcal{I}}^{(k)}) \end{cases},$$

from which we can easily notice that

$$(M + \epsilon)(\bar{\boldsymbol{\theta}} - \hat{\boldsymbol{\theta}}) = \begin{cases} 0, & \text{if } i \in \hat{\mathcal{A}} \setminus \mathcal{S}_{\mathcal{A}}^{(k)} \\ -\hat{\boldsymbol{d}}_i, & \text{if } i \in \mathcal{S}_{\mathcal{I}}^{(k)} \\ -(M + \epsilon)\hat{\boldsymbol{\theta}}_i, & \text{if } i \in \mathcal{S}_{\mathcal{A}}^{(k)} \\ 0, & \text{if } i \in \hat{\mathcal{I}} \setminus \mathcal{S}_{\mathcal{I}}^{(k)} \end{cases}. \quad (20)$$

Then, we can find that

$$\begin{aligned} \|(M + \epsilon)(\bar{\boldsymbol{\theta}} - \hat{\boldsymbol{\theta}}) + \hat{\boldsymbol{d}}\|^2 - \|\hat{\boldsymbol{d}}\|^2 &= \|(M + \epsilon)\hat{\boldsymbol{\theta}}_{\mathcal{S}_{\mathcal{A}}^{(k)}}\|^2 - \|\hat{\boldsymbol{d}}_{\mathcal{S}_{\mathcal{I}}^{(k)}}\|^2 \\ &\leq \|\rho_k^{-1}\hat{\boldsymbol{\theta}}_{\mathcal{S}_{\mathcal{A}}^{(k)}}\|^2 - \|\hat{\boldsymbol{d}}_{\mathcal{S}_{\mathcal{I}}^{(k)}}\|^2 \leq 0 \end{aligned}$$

where the first inequality holds because of $(M + \epsilon)^{-1} \in [\rho_k, \rho_{k+1})$ and the second inequality holds due to the definition of ρ_k . By decomposing the left-hand side of the above inequality and simple algebra, we have

$$(\bar{\boldsymbol{\theta}} - \hat{\boldsymbol{\theta}})^T \hat{\boldsymbol{d}} \leq -\frac{M + \epsilon}{2} \|\bar{\boldsymbol{\theta}} - \hat{\boldsymbol{\theta}}\|^2. \quad (21)$$

Next, we can establish an upper bound for $f(\bar{\boldsymbol{\theta}}) - f(\hat{\boldsymbol{\theta}})$:

$$\begin{aligned} f(\bar{\boldsymbol{\theta}}) - f(\hat{\boldsymbol{\theta}}) &\leq (\bar{\boldsymbol{\theta}} - \hat{\boldsymbol{\theta}})^T \hat{\boldsymbol{d}} + \frac{M}{2} \|\bar{\boldsymbol{\theta}} - \hat{\boldsymbol{\theta}}\|^2 \\ &\stackrel{(21)}{\leq} \frac{-\epsilon}{2} \|\bar{\boldsymbol{\theta}} - \hat{\boldsymbol{\theta}}\|^2 \\ &\stackrel{(20)}{=} \frac{-\epsilon \|\hat{\boldsymbol{d}}_{\mathcal{S}_{\mathcal{I}}^{(k)}}\|^2}{2(M + \epsilon)^2} - \frac{\epsilon \|\hat{\boldsymbol{\theta}}_{\mathcal{S}_{\mathcal{A}}^{(k)}}\|^2}{2} \\ &\leq \frac{-\epsilon \|\hat{\boldsymbol{d}}_{\mathcal{S}_{\mathcal{I}}^{(k)}}\|^2}{2(M + \epsilon)^2}. \end{aligned} \quad (22)$$

where the first inequality comes from the fact that f is M -RSS. Finally, since both $\tilde{\boldsymbol{\theta}}^{(k)}$ and $\bar{\boldsymbol{\theta}}$ have the support set $(\hat{\mathcal{A}} \setminus \mathcal{S}_{\mathcal{A}}^{(k)}) \cup \mathcal{S}_{\mathcal{I}}^{(k)}$, we have $f(\tilde{\boldsymbol{\theta}}^{(k)}) - f(\hat{\boldsymbol{\theta}}) \leq f(\bar{\boldsymbol{\theta}}) - f(\hat{\boldsymbol{\theta}})$ owing to the definition of $\tilde{\boldsymbol{\theta}}^{(k)}$. Coupled with (22), it leads to the conclusion of the Lemma 4.

Proof of Theorem 4. We reuse the notions in the proof of Lemma 3. We first show that the algorithm will not terminate if $\mathcal{A}^* \not\subseteq \hat{\mathcal{A}}$, i.e., $\mathcal{I}_1 = \mathcal{A}^* \setminus \hat{\mathcal{A}} \neq \emptyset$.

When $\mathcal{I}_1 \neq \emptyset$, we have:

$$\|\hat{\boldsymbol{\theta}} - \boldsymbol{\theta}^*\| \geq \frac{1}{\sqrt{2}} (\|\boldsymbol{\theta}_{\mathcal{I}_1}^*\| + \|\hat{\boldsymbol{\theta}}_{\mathcal{A}_2}\|) \geq \frac{1}{\sqrt{2}} (\vartheta + \|\hat{\boldsymbol{\theta}}_{\mathcal{A}_2}\|). \quad (23)$$

Then, we can establish an upper bound for $\|\hat{\boldsymbol{\theta}}_{\mathcal{A}_2}\|$ with $\frac{\sqrt{2}}{m} \|\hat{\boldsymbol{d}}_{\mathcal{I}_2^C}\|$:

$$\begin{aligned} \|\hat{\boldsymbol{d}}_{\mathcal{I}_2^C}\| &= \|\boldsymbol{d}_{\mathcal{I}_2^C}^* + \nabla_{\mathcal{I}_2^C}^2 f(\bar{\boldsymbol{\theta}})(\hat{\boldsymbol{\theta}}_{\mathcal{I}_2^C} - \boldsymbol{\theta}_{\mathcal{I}_2^C}^*)\| \\ &\geq m \|\hat{\boldsymbol{\theta}} - \boldsymbol{\theta}^*\| - \|\boldsymbol{d}_{\mathcal{I}_2^C}^*\| \\ &\stackrel{(23)}{\geq} \frac{m}{\sqrt{2}} \|\hat{\boldsymbol{\theta}}_{\mathcal{A}_2}\| + \frac{m}{\sqrt{2}} \vartheta - \sqrt{s + s^*} \|\boldsymbol{d}^*\|_{\infty} \\ &\geq \frac{m}{\sqrt{2}} \|\hat{\boldsymbol{\theta}}_{\mathcal{A}_2}\|, \end{aligned}$$

where $\bar{\boldsymbol{\theta}} = t\hat{\boldsymbol{\theta}} + (1-t)\boldsymbol{\theta}^*$, $0 \leq t \leq 1$, the last inequality comes from Assumption 4. Upon this inequality, we can show that

$$\max \{|\hat{\boldsymbol{d}}_i| : i \in \hat{\mathcal{I}}\} \geq \frac{1}{\sqrt{s^*}} \|\hat{\boldsymbol{d}}_{\mathcal{I}_1}\| = \frac{1}{\sqrt{s^*}} \|\hat{\boldsymbol{d}}_{\mathcal{I}_2^C}\| \geq \frac{m}{\sqrt{2s^*}} \|\hat{\boldsymbol{\theta}}_{\mathcal{A}_2}\| \geq m \sqrt{\frac{s - s^*}{2s^*}} \min\{|\hat{\boldsymbol{\theta}}_i| : i \in \hat{\mathcal{A}}\} \quad (24)$$

where the equality comes from the fact that $\hat{\boldsymbol{d}}_{\hat{\mathcal{A}}} = \mathbf{0}$ and the right-most inequality results from $|\mathcal{A}_2| = |\hat{\mathcal{A}} \cap \mathcal{I}^*| = s - |\hat{\mathcal{A}} \cap \mathcal{A}^*| \geq s - s^*$.

According to (24), we have

$$\frac{1}{m} \sqrt{\frac{2s^*}{s-s^*}} \geq \frac{\min \left\{ |\hat{\boldsymbol{\theta}}_i| : i \in \hat{\mathcal{A}} \right\}}{\max \left\{ |\hat{\mathbf{d}}_i| : i \in \hat{\mathcal{I}} \right\}} = \frac{\max \left\{ |\hat{\boldsymbol{\theta}}_i| : i \in \mathcal{S}_{\mathcal{A}}^{(1)} \right\}}{\min \left\{ |\hat{\mathbf{d}}_i| : i \in \mathcal{S}_{\mathcal{I}}^{(1)} \right\}} = \rho_1,$$

further, since $s > (1 + 2\frac{M^2}{m^2})s^*$, we have $\frac{1}{M} > \frac{1}{m} \sqrt{\frac{2s^*}{s-s^*}}$, and thus, $\frac{1}{M} > \rho_1$. Therefore, for $\forall \varepsilon > 0$, there exists $k \geq 1$ satisfying $\frac{1}{M+\varepsilon} \in [\rho_k, \rho_{k+1})$. By Lemma 4, for $\tilde{\boldsymbol{\theta}}^{(k)}$, it enjoys:

$$f(\tilde{\boldsymbol{\theta}}^{(k)}) - f(\hat{\boldsymbol{\theta}}) \leq \frac{-\varepsilon}{2(M_{s+s^*} + \varepsilon)^2} \|\nabla f(\hat{\boldsymbol{\theta}})_{\mathcal{S}_{\mathcal{I}}^{(k)}}\|^2 < 0,$$

which implies the algorithm shall not terminate.

Secondly, we will show that $\text{supp}(\boldsymbol{\theta}^*) = \text{supp}(\mathcal{H}_{s^*}(\hat{\boldsymbol{\theta}}))$ holds. To this end, it is equivalent to prove $\vartheta > \|\boldsymbol{\theta}^* - \mathcal{H}_{s^*}(\hat{\boldsymbol{\theta}})\|$, and we will prove this via constructing a contradiction.

Presume $\vartheta \leq \|\boldsymbol{\theta}^* - \mathcal{H}_{s^*}(\hat{\boldsymbol{\theta}})\|$, then according to Theorem 1 and Remark 2 of Shen and Li (2017), $\mathcal{H}_{s^*}(\hat{\boldsymbol{\theta}})$ satisfies a tight bound:

$$\|\boldsymbol{\theta}^* - \mathcal{H}_{s^*}(\hat{\boldsymbol{\theta}})\| \leq \frac{\sqrt{5}+1}{2} \|\boldsymbol{\theta}^* - \hat{\boldsymbol{\theta}}\|,$$

and hence, we can conclude that

$$\vartheta^{-1} \|\boldsymbol{\theta}^* - \hat{\boldsymbol{\theta}}\| \geq \frac{2}{\sqrt{5}+1}. \quad (25)$$

On the other hand, we have

$$\mathbf{0} = \nabla_{\hat{\mathcal{A}}} f(\hat{\boldsymbol{\theta}}) = \nabla_{\hat{\mathcal{A}}} f(\boldsymbol{\theta}^*) + \nabla_{\hat{\mathcal{A}}}^2 f(\bar{\boldsymbol{\theta}})(\hat{\boldsymbol{\theta}}_{\hat{\mathcal{A}}} - \boldsymbol{\theta}_{\hat{\mathcal{A}}}^*) + \nabla_{\hat{\mathcal{A}}} \nabla_{\mathcal{I}_1} f(\bar{\boldsymbol{\theta}})(-\boldsymbol{\theta}_{\mathcal{I}_1}^*) = \nabla_{\hat{\mathcal{A}}} f(\boldsymbol{\theta}^*) + \nabla_{\hat{\mathcal{A}}}^2 f(\bar{\boldsymbol{\theta}})(\hat{\boldsymbol{\theta}}_{\hat{\mathcal{A}}} - \boldsymbol{\theta}_{\hat{\mathcal{A}}}^*)$$

where $\bar{\boldsymbol{\theta}} = \lambda \boldsymbol{\theta}^* + (1-\lambda)\hat{\boldsymbol{\theta}}$ for $\lambda \in (0, 1)$, and the last inequality holds due to $\hat{\mathcal{A}} \supseteq \mathcal{A}^*$. Hence, we have

$$\|\boldsymbol{\theta}_{\hat{\mathcal{A}}}^* - \hat{\boldsymbol{\theta}}_{\hat{\mathcal{A}}}\| = \|\nabla_{\hat{\mathcal{A}}}^2 f(\bar{\boldsymbol{\theta}})^{-1} \mathbf{d}_{\hat{\mathcal{A}}}^*\| \leq \frac{1}{m} \|\mathbf{d}_{\hat{\mathcal{A}}}^*\| \leq \frac{\sqrt{s}}{m} \|\mathbf{d}^*\|_{\infty}, \quad (26)$$

Furthermore, owing to Assumption 4 and $\|\boldsymbol{\theta}^* - \hat{\boldsymbol{\theta}}\| = \|\boldsymbol{\theta}_{\hat{\mathcal{A}}}^* - \hat{\boldsymbol{\theta}}_{\hat{\mathcal{A}}}\|$, we can derive from (25) and (26) that

$$\frac{m}{2\sqrt{s+s^*}} > \vartheta^{-1} \|\mathbf{d}^*\|_{\infty} \geq \frac{m}{\sqrt{s}} \vartheta^{-1} \|\boldsymbol{\theta}^* - \hat{\boldsymbol{\theta}}\| \geq \frac{2m}{(\sqrt{5}+1)\sqrt{s}}.$$

However, we witness a contradiction between the left-most and right-most parts of this inequality. Therefore, $\vartheta > \|\boldsymbol{\theta}^* - \mathcal{H}_{s^*}(\hat{\boldsymbol{\theta}})\|$ holds, and we can claim $\text{supp}(\boldsymbol{\theta}^*) = \text{supp}(\mathcal{H}_{s^*}(\hat{\boldsymbol{\theta}}))$.

Proof of Theorem 5. Again, we use the notions in the proof of Theorem 1. Beside, we denote $\hat{\boldsymbol{\theta}} := \boldsymbol{\theta}^t$ and $\tilde{\boldsymbol{\theta}} := \boldsymbol{\theta}^{t+1}$. Let $\delta_4 = \frac{m_{s+s^*}}{4M_{s+s^*}} \left(1 - \frac{4s^*}{s-2s^*} \frac{M_{s+s^*}^2}{m_{s+s^*}^2}\right)$, $\varepsilon = \left(\frac{1}{2}\delta_4^{-1} \frac{m}{M} - 1\right)^{-1} M$, Lemma 4 ensures there is $k \in \{0, 1, \dots, s^*\}$ satisfying $\frac{1}{M+\varepsilon} \in [\rho_k, \rho_{k+1})$ such that $f(\tilde{\boldsymbol{\theta}}^{(k)}) - f(\hat{\boldsymbol{\theta}}) \leq \frac{-\varepsilon}{2(M+\varepsilon)^2} \|\hat{\mathbf{d}}_{\mathcal{S}_{\mathcal{I}}^{(k)}}\|^2 = -\frac{\delta_4}{m} (1 - 2\delta_4 \frac{M}{m}) \|\hat{\mathbf{d}}_{\mathcal{S}_{\mathcal{I}}^{(k)}}\|^2$.

We first consider the case that $k = s^*$. In this case, $|\mathcal{S}_{\mathcal{I}}^{(k)}| \geq |\mathcal{I}_1|$ holds, and thus $\|\hat{\mathbf{d}}_{\mathcal{S}_{\mathcal{I}}^{(k)}}\| \geq \|\hat{\mathbf{d}}_{\mathcal{I}_1}\|$ due to the definition of $\mathcal{S}_{\mathcal{I}}^{(k)}$. Therefore, we can show that

$$\begin{aligned}
& f(\hat{\boldsymbol{\theta}}) - f(\boldsymbol{\theta}^*) \\
& \leq \hat{\mathbf{d}}^\top (\hat{\boldsymbol{\theta}} - \boldsymbol{\theta}^*) - \frac{m}{2} \|\hat{\boldsymbol{\theta}} - \boldsymbol{\theta}^*\|^2 \\
& = \hat{\mathbf{d}}_{\mathcal{I}_2^C}^\top (\hat{\boldsymbol{\theta}} - \boldsymbol{\theta}^*)_{\mathcal{I}_2^C} - \frac{m}{2} \|\hat{\boldsymbol{\theta}}_{\mathcal{I}_2^C} - \boldsymbol{\theta}_{\mathcal{I}_2^C}^*\|^2 \\
& = \frac{1}{2m} \|\hat{\mathbf{d}}_{\mathcal{I}_2^C}\|^2 - \frac{m}{2} \|\hat{\boldsymbol{\theta}}_{\mathcal{I}_2^C} - \boldsymbol{\theta}_{\mathcal{I}_2^C}^*\|^2 - \frac{1}{m} \|\hat{\mathbf{d}}_{\mathcal{I}_2^C}\|^2 \\
& \leq \frac{\|\hat{\mathbf{d}}_{\mathcal{I}_2^C}\|}{2m} = \frac{\|\hat{\mathbf{d}}_{\mathcal{I}_1}\|}{2m} \\
& \leq \frac{\|\hat{\mathbf{d}}_{\mathcal{S}_{\mathcal{I}}^{(k)}}\|}{2m} \leq \frac{1}{2\delta_4(1 - 2\delta_4 \frac{M}{m})} (f(\hat{\boldsymbol{\theta}}) - f(\tilde{\boldsymbol{\theta}}^{(k)})).
\end{aligned} \tag{27}$$

It leads to:

$$\begin{aligned}
& f(\tilde{\boldsymbol{\theta}}^{(k)}) - f(\boldsymbol{\theta}^*) \\
& = f(\tilde{\boldsymbol{\theta}}^{(k)}) - f(\hat{\boldsymbol{\theta}}) + f(\hat{\boldsymbol{\theta}}) - f(\boldsymbol{\theta}^*) \\
& \leq [1 - 2\delta_4(1 - 2\delta_4 \frac{M}{m})] (f(\hat{\boldsymbol{\theta}}) - f(\boldsymbol{\theta}^*)) \\
& \leq (1 - \delta_4) (f(\hat{\boldsymbol{\theta}}) - f(\boldsymbol{\theta}^*)),
\end{aligned}$$

where the last inequality holds due to $\delta_4 < \frac{m}{4M}$ from the definition of δ_4 . With the above inequality and the fact that $f(\tilde{\boldsymbol{\theta}}) \leq f(\tilde{\boldsymbol{\theta}}^{(k)})$, we complete the proof for the first case.

Secondly, we turn to the case that $k + 1 \leq s^*$. Then, we give a lower bound for $\|\hat{\boldsymbol{\theta}} - \boldsymbol{\theta}^*\|$. It is easily notice that, $\|\hat{\boldsymbol{\theta}} - \boldsymbol{\theta}^*\| \geq \|\hat{\boldsymbol{\theta}}_{\mathcal{A}_{21}}\|$; and for $\|\hat{\boldsymbol{\theta}}_{\mathcal{A}_{21}}\|$, it satisfies

$$\begin{aligned}
\|\hat{\boldsymbol{\theta}}_{\mathcal{A}_{21}}\| & \geq \sqrt{|\mathcal{A}_{21}|} \max\{|\hat{\boldsymbol{\theta}}_i| : i \in \mathcal{S}_{\mathcal{A}}^{(k)}\} \\
& \geq \sqrt{s - 2s^*} \max\{|\hat{\boldsymbol{\theta}}_i| : i \in \mathcal{S}_{\mathcal{A}}^{(k)}\} \\
& = \sqrt{s - 2s^*} \rho_{k+1} \min\{|\hat{\mathbf{d}}_i| : i \in \mathcal{S}_{\mathcal{I}}^{(k)}\} \\
& \geq \sqrt{s - 2s^*} \rho_{k+1} |\mathcal{I}_{12}|^{-\frac{1}{2}} \|\hat{\mathbf{d}}_{\mathcal{I}_{12}}\| \\
& \geq \sqrt{\frac{s - 2s^*}{s^*}} \rho_{k+1} \|\hat{\mathbf{d}}_{\mathcal{I}_{12}}\| \\
& \geq \frac{1}{M + \varepsilon} \sqrt{\frac{s - 2s^*}{s^*}} \|\hat{\mathbf{d}}_{\mathcal{I}_{12}}\|,
\end{aligned}$$

where the first and second inequalities result from the definition of $\mathcal{S}_{\mathcal{A}}^{(k)}$ and $|\mathcal{A}_{21}| \geq s - 2s^*$, and the third and fourth equalities comes from the definition of $\mathcal{S}_{\mathcal{I}}^{(k)}$ and $|\mathcal{I}_{12}| \leq s^*$. Consequently, we have:

$$\frac{1}{M + \varepsilon} \sqrt{\frac{s - 2s^*}{s^*}} \|\hat{\mathbf{d}}_{\mathcal{I}_{12}}\| \leq \|\hat{\boldsymbol{\theta}} - \boldsymbol{\theta}^*\| \tag{28}$$

Let $l = 1 - 2\delta_4 \frac{M}{m}$ be a root of

$$\frac{m}{4l} - \frac{m}{2} + \frac{l}{m}(M + \varepsilon)^2 \frac{s^*}{s - 2s^*} = 0. \quad (29)$$

Then, we have

$$\begin{aligned} f(\hat{\boldsymbol{\theta}}) - f(\boldsymbol{\theta}^*) &\leq \hat{\mathbf{d}}_{\mathcal{I}_2^C}(\hat{\boldsymbol{\theta}} - \boldsymbol{\theta}^*)_{\mathcal{I}_2^C} - \frac{m}{2} \|\hat{\boldsymbol{\theta}}_{\mathcal{I}_2^C} - \boldsymbol{\theta}_{\mathcal{I}_2^C}^*\| \\ &= \left(\frac{m}{4l} - \frac{m}{2}\right) \|\hat{\boldsymbol{\theta}} - \hat{\boldsymbol{\theta}}^*\|^2 + \frac{l}{m} \|\hat{\mathbf{d}}_{\mathcal{I}_1}\|^2 - \left\| \sqrt{\frac{l}{m}} \hat{\mathbf{d}}_{\mathcal{I}_2^C} - \sqrt{\frac{m}{4l}} (\hat{\boldsymbol{\theta}} - \boldsymbol{\theta}^*)_{\mathcal{I}_2^C} \right\|^2 \\ &\leq \left(\frac{m}{4l} - \frac{m}{2}\right) \|\hat{\boldsymbol{\theta}} - \boldsymbol{\theta}^*\|^2 + \frac{l}{m} \|\hat{\mathbf{d}}_{\mathcal{I}_{12}}\|^2 + \frac{l}{m} \|\hat{\mathbf{d}}_{\mathcal{I}_{11}}\|^2 \\ &\leq \frac{l}{m} \|\hat{\mathbf{d}}_{\mathcal{S}_{\mathcal{I}}^{(k)}}\|^2 + \left(\frac{m}{4l} - \frac{m}{2}\right) \|\hat{\boldsymbol{\theta}} - \boldsymbol{\theta}^*\|^2 + \frac{l}{m} (M + \varepsilon)^2 \frac{s^*}{s - 2s^*} \|\hat{\boldsymbol{\theta}} - \boldsymbol{\theta}^*\|^2 \\ &= \frac{l}{m} \|\hat{\mathbf{d}}_{\mathcal{S}_{\mathcal{I}}^{(k)}}\|^2 \leq \frac{l}{\delta_4(1 - 2\delta_4 \frac{M}{m})} (f(\hat{\boldsymbol{\theta}}) - f(\tilde{\boldsymbol{\theta}}^{(k)})) \\ &= \delta_4^{-1} (f(\hat{\boldsymbol{\theta}}) - f(\tilde{\boldsymbol{\theta}}^{(k)})), \end{aligned}$$

where the second inequality holds owing to $\mathcal{I}_1 = \mathcal{I}_{12} \cup \mathcal{I}_{11}$, the third inequality holds because of (28) and the definition of $\mathcal{S}_{\mathcal{I}}^{(k)}$, the second equation holds because of (29). Upon this inequality, simple algebra shows that $f(\tilde{\boldsymbol{\theta}}^{(k)}) - f(\boldsymbol{\theta}^*) \leq (1 - \delta_4) (f(\hat{\boldsymbol{\theta}}) - f(\boldsymbol{\theta}^*))$. According to the definition of $\tilde{\boldsymbol{\theta}}$, we can easily derive that $f(\tilde{\boldsymbol{\theta}}) - f(\boldsymbol{\theta}^*) \leq (1 - \delta_4) (f(\hat{\boldsymbol{\theta}}) - f(\boldsymbol{\theta}^*))$. This completes the proof of the second part.

Proof of Theorem 6. Again, we use the notations in the proof of Theorem 5. Following the same derivation in (27), we have:

$$f(\hat{\boldsymbol{\theta}}) - f(\boldsymbol{\theta}^*) \geq \frac{m}{2} \|\hat{\boldsymbol{\theta}} - \boldsymbol{\theta}^*\|^2 - \|\mathbf{d}_{\mathcal{I}_2^C}^*\| \|\hat{\boldsymbol{\theta}} - \boldsymbol{\theta}^*\| = h(\|\hat{\boldsymbol{\theta}} - \boldsymbol{\theta}^*\|),$$

where $h(x) = \frac{m}{2}x^2 - \|\mathbf{d}_{\mathcal{I}_2^C}^*\|x$ is a quadratic function with respect to x .

Let $\delta_5 := (m\vartheta)^{-1} \sqrt{s + s^*} \|\mathbf{d}^*\|$, when $\hat{\mathcal{A}} \supseteq \mathcal{A}^*$, we have

$$\|\hat{\boldsymbol{\theta}} - \boldsymbol{\theta}^*\| \geq \|\boldsymbol{\theta}_{\mathcal{I}_1}^*\| \geq \vartheta = (m\delta_5)^{-1} \sqrt{s + s^*} \|\mathbf{d}^*\|_{\infty} \geq (m\delta_5)^{-1} \|\mathbf{d}_{\mathcal{I}_2^C}^*\| > m^{-1} \|\mathbf{d}_{\mathcal{I}_2^C}^*\|$$

we have $\nabla h(\|\hat{\boldsymbol{\theta}} - \boldsymbol{\theta}^*\|) = m\|\hat{\boldsymbol{\theta}} - \boldsymbol{\theta}^*\| - \|\mathbf{d}_{\mathcal{I}_2^C}^*\| > 0$. Consequently,

$$\begin{aligned} f(\hat{\boldsymbol{\theta}}) - f(\boldsymbol{\theta}^*) &\geq h(\vartheta) = \frac{m}{2} \vartheta^2 - \vartheta \|\mathbf{d}_{\mathcal{I}_2^C}^*\| \\ &\geq \left(\frac{1}{2} - \delta_5\right) m \vartheta^2 > 0 \end{aligned} \quad (30)$$

On the other hand, by recursively applying the result of Theorem 5, we can derive that, when $t \geq \log_{(1-\delta_4)^{-1}} \left[\frac{\max\{f(\boldsymbol{\theta}^0) - f(\boldsymbol{\theta}^*), 0\}}{(\frac{1}{2} - \delta_5) m \vartheta^2} \right]$, or equivalently

$$(1 - \delta_4)^t \max\{f(\boldsymbol{\theta}^0) - f(\boldsymbol{\theta}^*), 0\} < \left(\frac{1}{2} - \delta_5\right) m \vartheta^2,$$

we have

$$f(\boldsymbol{\theta}^t) - f(\boldsymbol{\theta}^*) \leq (1 - \delta_4)^t \max\{f(\boldsymbol{\theta}^0) - f(\boldsymbol{\theta}^*), 0\}.$$

Combining the two inequalities finally shows that $f(\hat{\boldsymbol{\theta}}) - f(\boldsymbol{\theta}^*) < \left(\frac{1}{2} - \delta_5\right) m \vartheta^2$. Compared with (30) when $\hat{\mathcal{A}} \subsetneq \mathcal{A}^*$, we can conclude that $\text{supp}(\boldsymbol{\theta}^t) \supseteq \mathcal{A}^*$ when $t \geq \log_{(1-\delta_4)^{-1}} \left[\frac{\max\{f(\boldsymbol{\theta}^0) - f(\boldsymbol{\theta}^*), 0\}}{(\frac{1}{2} - \delta_5) m \vartheta^2} \right]$.

5. Applications

In this section, we aim to demonstrate the universality of Algorithm 1 by applying it to several benchmarked sparse learning tasks in statistical machine learning. These tasks include compressed sensing, learning sparse classifiers, and reconstructing binary pairwise Markov networks. See Sections 5.1, 5.2, and 5.3, respectively. For these tasks, we will verify Assumptions in Section 3.1 under widely accepted conditions in literature so as to ensure that the solution can be quickly offered by Algorithm 1 and enjoys admirable properties. Note that the verification of Assumptions 3-4 follows a similar procedure by modifying conditions accordingly, and thus, it will be omitted for reader's exercises.

5.1. Compressed Sensing

Standard compressed sensing problems aim to estimate the a s -sparse vector $\boldsymbol{\theta}^*$ from noisy linear measurements \mathbf{y} that comes from the linear model: $\mathbf{y} = \mathbf{X}\boldsymbol{\theta}^* + \boldsymbol{\epsilon}$,

where $\mathbf{X} \in \mathbb{R}^{n \times p}$ is a known sensing matrix, $\boldsymbol{\epsilon} = (\epsilon_1, \dots, \epsilon_n)^\top$ is the additive measurement noise, and $\epsilon_1, \dots, \epsilon_n$ are *i.i.d.* zero-mean random noises. Under the linear model, compressed sensing is formulated as a sparsity-constraint problem (2) in which the objective function $f(\boldsymbol{\theta}) = \|\mathbf{y} - \mathbf{X}\boldsymbol{\theta}\|^2$. Since f is a convex function with twice differentiation, we can directly apply Algorithm 1 to obtain an estimator $(\hat{\boldsymbol{\theta}}, \hat{\mathcal{A}})$ for $(\boldsymbol{\theta}^*, \mathcal{A}^*)$.

Next, we give a theoretical analysis to confirm that the estimator enjoys admirable statistical properties and can be quickly returned by Algorithm 1. We achieve this by verifying Assumptions in Section 3.1 under certain conditions. The conditions are listed as follows.

(A1) There exists constants $0 < m_{3s} < M_{3s} \leq 1.49m_{3s} < \infty$ such that $\forall \mathcal{A} \subseteq \{1, 2, \dots, p\}$ with $|\mathcal{A}| \leq 3s$ and $\forall \mathbf{u} \in \mathbb{R}^{|\mathcal{A}|}$, we have: $m_{3s}\|\mathbf{u}\|^2 \leq \frac{1}{n}\|\mathbf{X}_{\mathcal{A}}\mathbf{u}\|^2 \leq M_{3s}\|\mathbf{u}\|^2$.

(A2) For each $i \in [n]$, ϵ_i is a sub-Gaussian random variable with parameter σ , i.e., for all $t \geq 0$, we have: $\mathbb{P}\{|\epsilon_i| \geq t\} \leq 2\exp(-t^2/\sigma^2)$.

Condition (A1) refers to the sparse Riesz condition in the literature for the analysis of sparse generalized linear models, which serves as an identifiability condition for support recovery (Zhang and Huang 2008, Shen et al. 2012). Besides, as we have discussed in Section 3.1, $M_{3s} \leq 1.49m_{3s}$ is the widely accepted RIP-type condition for learning sparse linear model. Condition (A2) is a standard assumption in literature (Wainwright 2019). It ensures that the probability of deviation from zero decays exponentially fast.

We begin to confirm Assumptions 1 and 2 hold wherein we assume $\mathbf{x}_i^\top \mathbf{x}_i = n$ for every $i \in [p]$ to facilitate the analyses. First, for any $\boldsymbol{\theta}, \boldsymbol{\theta}'$ such that $|\text{supp}(\boldsymbol{\theta} - \boldsymbol{\theta}')| \leq 3s$, we have:

$$\frac{m_{3s}}{2}\|\boldsymbol{\theta}' - \boldsymbol{\theta}\|^2 \leq f(\boldsymbol{\theta}') - f(\boldsymbol{\theta}) - \nabla f(\boldsymbol{\theta})^\top (\boldsymbol{\theta}' - \boldsymbol{\theta}) = \frac{1}{2n}\|\mathbf{X}(\boldsymbol{\theta}' - \boldsymbol{\theta})\|^2 \leq \frac{M_{3s}}{2}\|\boldsymbol{\theta}' - \boldsymbol{\theta}\|^2$$

due to Condition (A1). Therefore, Assumption 1 holds. Second, we have $n\|\nabla f(\boldsymbol{\theta}^*)\|_\infty = \|\mathbf{X}^\top \boldsymbol{\epsilon}\|_\infty = \max_{1 \leq i \leq p} |\mathbf{X}_i^\top \boldsymbol{\epsilon}|$. Owing to Condition (A2), $\mathbf{X}_i^\top \boldsymbol{\epsilon}$ is a sub-Gaussian random variable with parameter $\sqrt{n}\sigma$ (Wainwright 2019). Then, simple algebra can show that for the constant $c = 1.49m_{3s} - M_{3s} \geq 0$,

$$\begin{aligned} \mathbb{P}(\|\nabla f(\boldsymbol{\theta}^*)\|_\infty \geq c\vartheta) &= \mathbb{P}\left(n^{-1} \max_{i \in [p]} |\mathbf{X}_i^\top \boldsymbol{\epsilon}| \geq c\vartheta\right) \\ &\leq p\mathbb{P}\left(|\mathbf{X}_i^\top \boldsymbol{\epsilon}| \geq nc\vartheta\right) \leq 2p \exp\left(-\frac{nc^2\vartheta^2}{2\sigma^2}\right). \end{aligned}$$

Consequently, Assumption 2 holds with probability at least $1 - 2\exp\{\log p - \frac{nc^2\vartheta^2}{2\sigma^2}\}$.

In summary, when Conditions (A1)-(A2), Theorem 1 ensures $\text{supp}(\hat{\mathcal{A}}) = \text{supp}(\mathcal{A}^*)$ with high probability. In particular, if $\vartheta = O(\sqrt{\log p/n})$, the probability of $\text{supp}(\hat{\mathcal{A}}) = \text{supp}(\mathcal{A}^*)$ converges to 1 as $n \rightarrow \infty$. Furthermore, Theorem 3 shows that, with high probability, Algorithm 1 terminate after $O\left(\log_{\delta_1}\left(\frac{\|f(\boldsymbol{\theta}^0) - \|\boldsymbol{\epsilon}\|\|}{\delta_2 m_{3s} \vartheta}\right)\right)$ splicing iteration. Since each splicing iteration takes $O(snp)$ time complexity, the total time complexity of Algorithm 1 is $O\left(snp\left(\log_{\delta_1}\left(\frac{\|f(\boldsymbol{\theta}^0) - \|\boldsymbol{\epsilon}\|\|}{\delta_2 m_{3s} \vartheta}\right)\right)\right)$.

5.2. Sparse Classifier

Finding the core elements to classify the objects is a crucial application task and attracts much attention from the statistical learning community. The logistic regression model is an important model to solve this problem, which leverages the information of explanatory variables $\mathbf{x} \in \mathbb{R}^p$ to predict the class of response variable $y \in \{0, 1\}$. The underlying logistic regression model is expressed as follows:

$$\mathbb{P}(y = 1 \mid \mathbf{x}) = \frac{\exp(\mathbf{x}^\top \boldsymbol{\theta}^*)}{1 + \exp(\mathbf{x}^\top \boldsymbol{\theta}^*)}, \quad (31)$$

where $\boldsymbol{\theta}^* \in \mathbb{R}^p$ is an unknown s -sparse vector that to be estimated.

We want to estimate $\boldsymbol{\theta}^*$ by collecting n independent samples of the explanatory variables and the response variable that are stored into $\mathbf{X} = (\mathbf{x}_1, \dots, \mathbf{x}_n)^\top \in \mathbb{R}^{n \times p}$ and $\mathbf{y} = (y_1, \dots, y_n) \in \mathbb{R}$. With these samples, we estimate $\boldsymbol{\theta}^*$ by minimizing the negative log-likelihood under sparsity constraint $\arg \min_{\boldsymbol{\theta} \in \mathbb{R}^p, f(\boldsymbol{\theta})} \text{s.t. } \|\boldsymbol{\theta}\|_0 \leq s$, where

$$f(\boldsymbol{\theta}) := -\frac{1}{n} \sum_{i=1}^n \{y_i \mathbf{x}_i^\top \boldsymbol{\theta} - b(\mathbf{x}_i^\top \boldsymbol{\theta})\}$$

and $b(t) = \log(1 + \exp(t))$. We can apply Algorithm 1 on this task to solve $(\hat{\boldsymbol{\theta}}, \hat{\mathcal{A}})$ because $f(\cdot)$ has the second differentiation.

Next, we show that, under some reasonable conditions, Algorithm 1 completes iterations quickly, and its output enjoys statistical guarantees. The conditions are presented below.

(B1) The same as Condition (A1) in Section 5.1.

(B2) There exists a positive constant δ satisfying $\frac{M_{3s}}{5.96m_{3s}} \leq \delta \leq \min_{i \in [n]} \nabla^2 b(\mathbf{x}_i^\top \check{\boldsymbol{\theta}})$ for any $3s$ -sparse vector $\check{\boldsymbol{\theta}}$ such that $f(\check{\boldsymbol{\theta}}) < f(\boldsymbol{\theta}^0)$.

The upper bound for δ in Condition (B2) restricts \mathbf{y}_i cannot be a degenerate random variable to avoid infinitely small variances (Rigollet 2012) so as to ensure the objective function being strongly convex. This assumption is also introduced in Yuan et al. (2017, 2020). The lower bound condition on δ is a RIP-type condition for $\frac{M_{3s}}{m_{3s}}$ under logistic regression.

We verify Assumptions 1-2 with Conditions (B1)-(B2). Without loss of generality, we assume $\|\mathbf{x}_j\| = \sqrt{n}$. First, we verify RSC and RSS of $f(\cdot)$. According to Taylor-series expansion, for $\forall \boldsymbol{\theta}, \boldsymbol{\theta}'$ with $\|\boldsymbol{\theta} - \boldsymbol{\theta}'\|_0 \leq 3s$, we have:

$f(\boldsymbol{\theta}') - f(\boldsymbol{\theta}) - \nabla f(\boldsymbol{\theta})^\top (\boldsymbol{\theta}' - \boldsymbol{\theta}) = \frac{1}{2n} \|H(\mathbf{X}, \bar{\boldsymbol{\theta}}) \mathbf{X}(\boldsymbol{\theta}' - \boldsymbol{\theta})\|^2$, where $H(\mathbf{X}, \bar{\boldsymbol{\theta}}) = \text{diag} \left\{ \sqrt{\nabla^2 b(\mathbf{x}_1^\top \bar{\boldsymbol{\theta}})}, \dots, \sqrt{\nabla^2 b(\mathbf{x}_n^\top \bar{\boldsymbol{\theta}})} \right\}$ and $\bar{\boldsymbol{\theta}} = \lambda \boldsymbol{\theta} + (1 - \lambda) \boldsymbol{\theta}'$ for some $\lambda \in (0, 1)$. Then, by Conditions (B1) and (B2) together with the fact that $\nabla^2 b(t) \leq \frac{1}{4}$, we have:

$$\begin{aligned} \frac{1}{2n} \|H(\mathbf{X}, \bar{\boldsymbol{\theta}}) \mathbf{X}(\boldsymbol{\theta}' - \boldsymbol{\theta})\|^2 &\leq \frac{1}{8n} \|\mathbf{X}(\boldsymbol{\theta}' - \boldsymbol{\theta})\|^2 \leq \frac{M_{3s}}{8} \|\boldsymbol{\theta}' - \boldsymbol{\theta}\|^2, \\ \frac{1}{2n} \|H(\mathbf{X}, \bar{\boldsymbol{\theta}}) \mathbf{X}(\boldsymbol{\theta}' - \boldsymbol{\theta})\|^2 &\geq \frac{\delta}{2n} \|\mathbf{X}(\boldsymbol{\theta}' - \boldsymbol{\theta})\|^2 \geq \frac{\delta m_{3s}}{2} \|\boldsymbol{\theta}' - \boldsymbol{\theta}\|^2. \end{aligned}$$

Thus, $f(\boldsymbol{\theta})$ is $\frac{M_{3s}}{4}$ -RSS and

$\frac{m_{3s}}{5.96}$ -RSC. Next, for the gradient at $\boldsymbol{\theta}^*$, it has the form $\nabla f(\boldsymbol{\theta}^*) = (g_1, \dots, g_p)$, where $g_j = \frac{1}{n} \sum_{i=1}^n (\nabla b(\mathbf{x}_i^\top \boldsymbol{\theta}^*) - \mathbf{y}_i) \mathbf{x}_{ij}$. Since $(\nabla b(\mathbf{x}_i^\top \boldsymbol{\theta}^*) - \mathbf{y}_i) \mathbf{x}_{ij}$ is a zero-mean random variable with range $[-\mathbf{x}_{ij}, \mathbf{x}_{ij}]$, then g_j satisfies $\mathbb{P}(|g_j| > c\vartheta) \leq 2 \exp\{-\frac{c^2 \vartheta^2 n}{2}\}$ according to Hoeffding's inequality for general bounded random variables where $c = \frac{0.35}{\sqrt{s}} (1.49 \delta m_{3s} - \frac{M_{3s}}{4}) > 0$ (because of Condition (B1)). Consequently, it results in $\mathbb{P}(\|\nabla f(\boldsymbol{\theta}^*)\|_\infty \geq c\vartheta) \leq 2 \exp\left\{\log p - \frac{nc^2 \vartheta^2}{2}\right\}$, which means Assumption 2 holds with high probability. And hence, with Conditions (B1)-(B2), we can deduce $\text{supp}\{\hat{\boldsymbol{\theta}}\} = \mathcal{A}^*$ holds with probability at least $1 - 2 \exp\left\{\log p - \frac{nc^2 \vartheta^2}{2}\right\}$. When $\vartheta = O(\sqrt{\log p/n})$, we can see that $\mathbb{P}(\text{supp}\{\hat{\boldsymbol{\theta}}\} = \mathcal{A}^*)$ reaches 1 as n goes to infinity.

5.3. Sparse Ising model

The Ising model is a powerful undirected graphical model for characterizing pairwise interactions between binary random variables, which is widely used in many fields such as neuroscience, ecology, and sociology.

Precisely, let $\mathbf{x} = (x_1, \dots, x_p)^\top \in \{-1, 1\}^p$ be a set of binary random variables, then Ising model at \mathbf{x} has probability: $\mathbb{P}(\mathbf{x}) = \frac{1}{\Phi(\boldsymbol{\theta}^*)} \exp\left\{\frac{1}{2} \sum_{k,l=1}^p \boldsymbol{\theta}_{kl}^* x_k x_l\right\}$,

where $\boldsymbol{\theta}^* \in \mathbb{R}^{p \times p}$ is a zero-diagonal symmetric matrix whose non-diagonal entries represent the strength of pairwise interactions of variables, and $\Phi(\boldsymbol{\theta}^*) = \sum_{\mathbf{z} \in \{-1, 1\}^p} \exp\left\{\frac{1}{2} \sum_{k,l=1}^p \boldsymbol{\theta}_{kl}^* z_k z_l\right\}$ is a normalization constant. It is worth noting that, in the Ising model, variables k and l are connected by an edge if $\boldsymbol{\theta}_{kl}^* \neq 0$. Therefore, $\boldsymbol{\theta}^*$ corresponds to an interaction network for variables x_1, \dots, x_p . From intuition, each variable in the interaction network only connects to a few variables; thus, the interaction network should be sparse. To rephrase, $\boldsymbol{\theta}^*$ is a sparse matrix to be recovered.

To this end, given n samples $\mathbf{X} = (\mathbf{x}_1, \dots, \mathbf{x}_n)^\top \in \{-1, 1\}^{n \times p}$, we can minimize the negative log-likelihood with the constraint of non-zero entries in the upper diagonal matrix:

$$\arg \min_{\boldsymbol{\theta} \in \mathcal{S}_p} -\frac{1}{n} \sum_{i=1}^n \log(\mathbb{P}(\mathbf{x}_i)), \text{ s.t. } \|\boldsymbol{\theta}\|_0 \leq s,$$

where \mathcal{S}_p is the space of p -by- p zero-diagonal symmetric matrix and $\|\boldsymbol{\theta}\|_0 = \sum_{k < l} \mathbf{I}(\boldsymbol{\theta}_{kl} \neq 0)$. However, it is intractable to compute the negative log-likelihood because $\Phi(\boldsymbol{\theta})$ is the sum of 2^p elements. To circumvent this difficulty, we use the pseudo-likelihood as an alternative objective:

$$\arg \min_{\boldsymbol{\theta} \in \mathcal{S}_p} f(\boldsymbol{\theta}) := -\frac{1}{n} \sum_{i=1}^n \log \left[\prod_{k=1}^p \mathbb{P}(\mathbf{x}_{ik} | \mathbf{x}_{i1}, \dots, \mathbf{x}_{ik-1}, \mathbf{x}_{ik+1}, \dots, \mathbf{x}_{ip}) \right], \text{ s.t. } \|\boldsymbol{\theta}\|_0 \leq s.$$

The pseudo-likelihood is widely used in literature for learning the Ising model (Höfling and Tibshirani 2009, Xue et al. 2012) because it has admirable properties in both computing and statistics: (i) it can be computed in $O(np)$ times; (ii) it is a twice-differentiable convex function; (iii) it well approximates the likelihood when the Ising model is sparse. With these advantages, Algorithm 1 can be efficiently conducted upon the pseudo-likelihood and returns $(\hat{\boldsymbol{\theta}}, \hat{\mathcal{A}})$.

To assure the theoretical guarantees of Algorithm 1, we certify Assumptions in Section 3.1 hold under following conditions:

- (C1) For $\forall \mathcal{A} \subseteq [p]$ with $|\mathcal{A}| \leq \min\{3s, p-1\}$, there exist constants $0 < m_{3s} < M_{3s} < \infty$ such that $nm_{3s}\|\mathbf{u}\|^2 \leq \|\mathbf{X}_{\mathcal{A}}\mathbf{u}\|^2 \leq nM_{3s}\|\mathbf{u}\|^2$, for $\forall \mathbf{u} \in \mathbb{R}^{|\mathcal{A}|}$.
- (C2) For some constant $\omega > 0$, any $3s$ -sparse vector $\check{\boldsymbol{\theta}}$ such that $f(\check{\boldsymbol{\theta}}) < f(\boldsymbol{\theta}_0)$ satisfies $\max_{l \in [p]} \sum_{k \neq l} |\check{\boldsymbol{\theta}}_{kl}| \leq \omega$ and $\frac{1+M_{3s}}{11.92(1+m_{3s})} < \Delta$ where $\Delta = \frac{e^{2\omega}}{(e^{2\omega}+1)^2}$.

When $3s < p-1$, Condition (C1) is identical to Condition (B1) and can be interpreted similarly. This condition also implies that when $p > n$, s cannot exceed $O(p)$, which is reasonable because the collected data is limited. On the other hand, if $n > p$, Condition (C1) can hold even when $|\mathcal{A}| = p-1$ once the correlation among variables is bounded. The upper bound for $\max_{l \in [p]} \sum_{k \neq l} |\check{\boldsymbol{\theta}}_{kl}|$ in Condition (C2) is to avoid the case when one binary variable can be perfectly predicted, at which randomness does not exist. This upper bound is widely imposed to ensure the identifiability of the sparse Ising model (Santhanam and Wainwright 2012, Lohov et al. 2018). Besides, the bound for $\frac{1+M_{3s}}{1+3m_{3s}}$ is a RIP-type condition under Ising model.

The following Proposition shows that $f(\cdot)$ satisfies Assumption 1.

PROPOSITION 1. *Under Conditions (C1) and (C2), $f(\cdot)$ is $8\Delta(1+m_{3s})$ -RSC and $(1+M_{3s})$ -RSS.*

Then, we give an upper bound for $\|\nabla f(\boldsymbol{\theta}^*)\|_\infty := \max_{k, l \in [p]} (\nabla f)_{kl}$. For $\forall k, l \in [p]$ satisfying $k \neq l$, we have $-2\mathbf{x}_{ik}\mathbf{x}_{il}(2 - \phi_k(\mathbf{x}_i) - \phi_l(\mathbf{x}_i)) \in [-4, 4]$ for each i . Thus, its independent empirical mean $(\nabla f(\boldsymbol{\theta}^*))_{kl}$ is a sub-Gaussian variable with parameter $\frac{4}{\sqrt{n}}$ by Hoeffding's inequality. According to Condition (C2), we can define a positive value $c = \frac{0.35}{\sqrt{s}}(11.92\Delta(1+m_{3s}) - (1+M_{3s}))$, then owing to $\mathbb{E}[\nabla f(\boldsymbol{\theta}^*)] = \mathbf{0}$ (Xue et al.

2012), we have $\mathbb{P}(\|\nabla f(\boldsymbol{\theta}^*)\|_\infty \geq c\vartheta) \leq 2 \exp\left\{\log \frac{p(p-1)}{2} - \frac{nc^2\vartheta^2}{8}\right\}$, implying Assumption 2 holds with high probability. Particularly, when $\vartheta = O(\sqrt{\log p/n})$, Assumption 2 holds with probability 1 as $n \rightarrow \infty$; subsequently, the properties of SCOPE hold with probability 1. It means that SCOPE can exactly recover the underlying graph structure of the Ising model with probability one within a few iterations.

6. Numerical experiments

In this section, we evaluate the empirical performance of the SCOPE algorithm with two numerical experiments. The first experiment aims to illustrate the support recovery property and computational merits of our algorithm by comparing it with the exact solver (see Section 6.1). The second experiment demonstrates the empirical advantages of our method against the state-of-the-art algorithms (see Section 6.2).

6.1. Comparisons with the exact solver

Here, we select a commercial MIO solver, GUROBI (Gurobi Optimization, LLC 2022), for comparison because it is one of the most popular solvers for sparse-constrained optimization. We will compare SCOPE with GUROBI on problem (2). We select problem (2) as our benchmark because it is well-developed and supported by GUROBI.

We depict the detailed numerical settings for problem (2) in the following. Specifically, we create noisy linear measurements \mathbf{y} that comes from the underlying linear model with a s -sparse parameter vector $\boldsymbol{\theta}^*$: $\mathbf{y} = \mathbf{X}\boldsymbol{\theta}^* + \boldsymbol{\epsilon}$, where $\boldsymbol{\epsilon} = (\epsilon_1, \dots, \epsilon_n)^\top$ is the additive measurement noise, and $\epsilon_1, \dots, \epsilon_n$ are *i.i.d.* zero-mean random noises. First, we generate a random predictor matrix $\mathbf{X} \in \mathbb{R}^{n \times p}$ whose row vectors $\mathbf{X}_1, \dots, \mathbf{X}_n$ are *i.i.d.* $\mathcal{N}(\mathbf{0}, \boldsymbol{\Sigma})$, where the (i, j) -entry of covariance matrix is $\Sigma_{ij} = \rho^{|i-j|}$. Here, we set $\rho = 0.6$. In terms of the s -sparse regression coefficients $\boldsymbol{\theta}^*$, the indices of its non-zero entries are randomly selected from $[p]$, and their values are selected from $\{-100, 100\}$ with equal chance. As for the random noise $\boldsymbol{\epsilon}$, it is sampled from $\mathcal{N}(\mathbf{0}, \sigma^2 \mathbf{I}_{p \times p})$ such that the signal-to-noise ratio $\|\mathbf{X}\boldsymbol{\theta}^*\|^2/\sigma^2$ is equal to 1. Finally, the response is generated according to the above linear model, and it is adjusted to have a zero mean and a variance of one for normalization purposes.

We measure the empirical performance of algorithms by the proportion of non-zero entries that are correctly selected. To evaluate the computational performance, we measure each algorithm's running time (measured in seconds). We investigate both support recovery accuracy and computational behavior in the cases where sample size n , dimension p , and sparsity s vary, but the remaining are fixed. The results are summarized in Figure 1.

The left-upper panel of Figure 1 shows that both SCOPE and GUROBI can recover the support with perfect accuracy when the sample size is more than 800. Besides, we can see that SCOPE and GUROBI have a very close performance. In terms of runtime performance presented in the right-upper panel of Figure 1, the runtime of GUROBI is more than one second in most cases and its runtime would increase when it

has a lower probability of identifying the true support set. On the contrary, SCOPE can finish iterations in one-tenth of a second in most cases.

Next, we turn to the results when p varies, but n, s are fixed (presented in the middle panel of Figure 1). We can first see that both SCOPE and GUROBI have a higher support recovery accuracy when p decreases. And they have a very similar performance in most cases. From the right-middle panel of Figure 1, the runtime of GUROBI quickly grows as p increases while the runtime of SCOPE grows slowly. Thus, SCOPE still shows dominant runtime advantages — it converges in less than one second when $p = 100$, but GUROBI has reached its time limit. Finally, as we can see in the left-bottom of Figure 1, an increasing s makes the sparsity optimization harder, and thus, both GUROBI and SCOPE have lower accuracy. The SCOPE seems to be better when $s \geq 6$, and it maintains a competitive performance in other cases. In all, the gap between GUROBI and SCOPE is still tiny. The main difference between them lies in the runtime presented in the right-bottom panel of Figure 1. GUROBI has a sharp-growth runtime concerning s . As for SCOPE, its runtime grows much slower and can converge in less than one second.

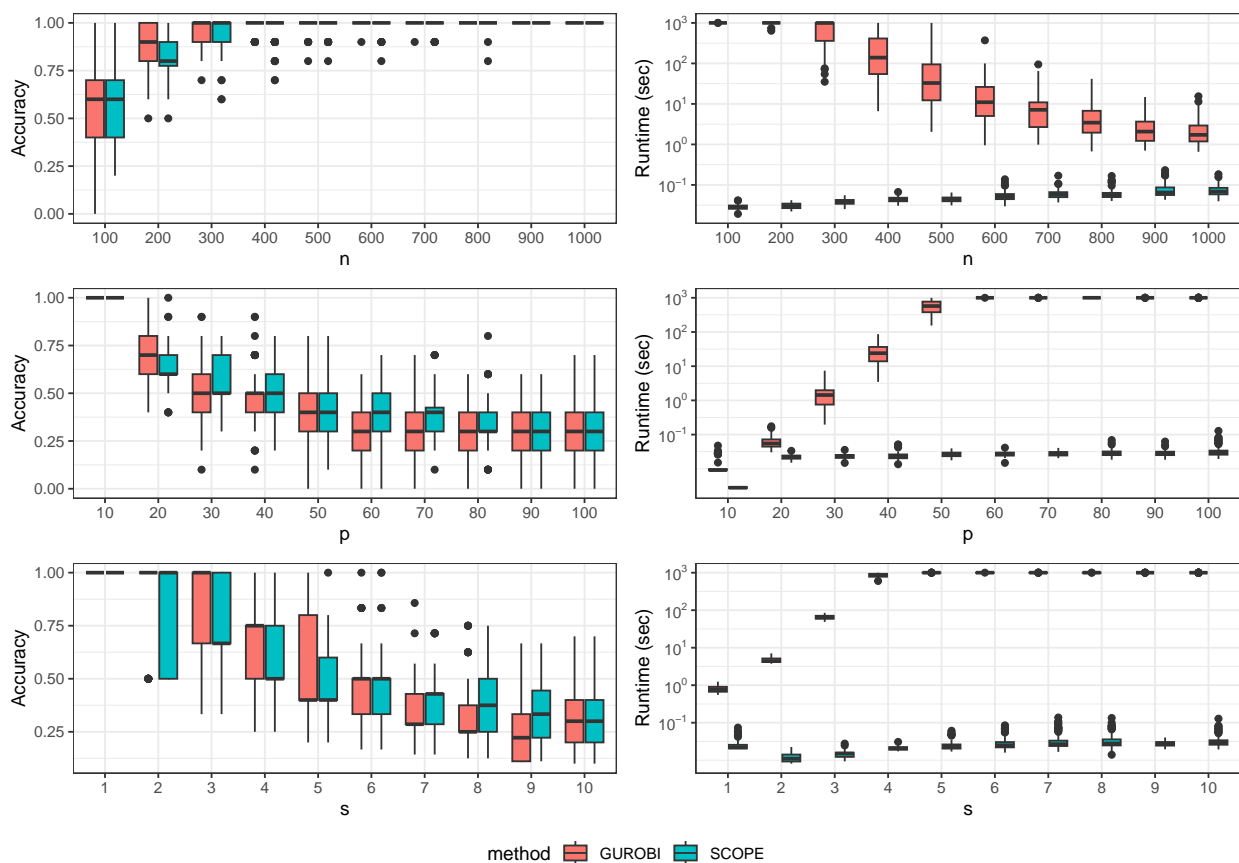


Figure 1 The boxplot of accuracy (Left panel) and runtime (Right panel). Upper panel: n increases when p and s is fixed at $p = 100$ and $s = 10$; Middle panel: p increases when fixing $n = 50, s = 10$; Bottom panel: increasing s but fixing $n = 50, p = 100$. Note that the runtime of the two methods is limited to 1000 seconds. The experiment was independently repeated 100 times.

6.2. Comparisons with State-of-the-Art Methods

Here, we compare our algorithm with the other competitive methods in the literature. We list the competitors below with descriptions for their implementation.

- Lasso-type regularization method. We use the `cvxpy` Python package (Diamond and Boyd 2016) to get the solution of the convex relaxation of (1): $\arg \min_{\theta \in \mathbb{R}^p} f(\theta)$, s.t. $\|\theta\|_1 \leq \lambda$, where λ is a fixed regularization strength (Tibshirani 1996, Park and Hastie 2007, Höfling and Tibshirani 2009). Since there is no explicit expression that can determine s from λ , we will consider multiple values for λ and find out the one that results in a s -sparse parameter estimation.
- Gradient support pursuit (GraSP).
- Gradient hard thresholding pursuit (GraHTP). We consider two methods for deciding the step size used in GraHTP. One method uses a fixed step size $(2M_{2s})^{-1}$ as suggested by Theorem 5 in Yuan et al. (2017). Since it is difficult to exactly compute M_{2s} , we approximate M_{2s} with the largest singular value of $\nabla_{\mathcal{A}_0}^2 f(\theta_0)$ for instead. Another method considers five step sizes $10^0, 10^{-1}, \dots, 10^{-4}$. For each step size, we run GraHTP and record the objective when it converges. Then we choose the step size that gives the smallest objective. The two methods are denoted as GraHTP1 and GraHTP2, respectively.

We will systematically compare these methods in learning sparse linear, sparse classification, and sparse Ising models. The model settings are summarized below.

- **Linear model.** We adopt the settings depicted in the second paragraph on Section 6.1 except the signal-to-noise ratio is set as 6.
- **Classification model.** We inherit the settings for \mathbf{X} and θ^* from the linear model in the previous section. The only difference is that the response y_i is sampled from a binomial variable with probability (31).
- **Ising model.** First, we depict the method for generating $\theta^* \in \mathbb{R}^{p \times p}$: (i) generate a zero-diagonal upper-triangle matrix $\mathbf{S} \in \mathbb{R}^{p \times p}$ whose s non-zero entries are randomly selected from upper triangle; (ii) for the non-zero entries in \mathbf{S} , their values are randomly drawn from $\{-0.5, 0.5\}$ with equal probability; (iii) $\theta = \mathbf{S}^\top + \mathbf{S}$. Then, we independently draw n samples from the Ising model in Section 5.3.

For the linear model and classification model, we set $p = 500$ and $s = 50$; as for the Ising model, we set $p = 20$, and $s = 40$. We adopt the same evaluation metrics in Section 6.1. The numerical results of the three models are demonstrated in Figure 2.

Figure 2 shows that, among these methods, SCOPE uses the minimal samples to perfectly recover \mathcal{A}^* in the three models. The results also verify the support recovery property of SCOPE in Theorem 1. Like SCOPE, GraHTP2 can recover \mathcal{A}^* in all of the three models since it has a support recovery guarantee when its hyperparameter, step size, is properly chosen. However, when step size is not chosen appropriately, GraHTP may not correctly recover \mathcal{A}^* when the sample size is large, which can be witnessed by the performance of GraHTP1. In contrast to GraHTP2, GraHTP1 fails to recover \mathcal{A}^* in logistic regression and

Ising model when $n \geq 600$ regardless of its successful recovery for \mathcal{A}^* in the linear model. These numerical results suggest tuning the hyperparameter is essential for GraHTP. In terms of GraSP, despite it having no support recovery guarantee, it can successfully identify \mathcal{A}^* under the linear model and Ising regression model, and its accuracy is very close to 1 under logistic regression. Yet, compared with the SCOPE, it generally requires more samples to recover \mathcal{A}^* in these models. Finally, the Lasso-based relaxation method, it can recover \mathcal{A}^* in all models, as the theory suggests. Unfortunately, it requires more samples to reach perfect recovery compared to SCOPE.

From the runtime analysis presented in the bottom panel of Figure 2, it is evident that SCOPE exhibits significant computational advantages compared to other methods. In particular, when compared to GraSP and GraHTP2, which accurately recover the support set in all three models, SCOPE achieves a speedup of 20-100 times. Furthermore, our computation speed is 10-20 times faster than Lasso-based methods. In most cases, SCOPE outperforms GraHTP1 in terms of speed. Although it is worth noting that GraHTP1 achieves faster computation under logistic regression when the sample size is large, it does so at the expense of reduced support-set-recovery accuracy. The computational efficiency of SCOPE can be attributed to two factors: (i) our careful algorithmic design and (ii) the effective implementation of our algorithm in C++. In summary, these numerical results clearly demonstrate that our method is well-suited for large-scale sparse optimization problems and can be considered a primary choice for these problems.

7. Conclusion

Motivated by the splicing technique introduced in Zhu et al. (2020), this paper proposes the SCOPE algorithm for solving (1). Under sufficient conditions, the algorithm recovers the true support set in a linear convergence rate. Impressively, these theoretical guarantees are attained without tuning hyper-parameters. To the best of our knowledge, SCOPE is the first tuning-free algorithm for (1). The numerical results show that, in most cases, SCOPE surpasses state-of-the-art solvers in terms of both accuracy and computational efficiency.

Acknowledgments

Wang’s research is partially supported by National Natural Science Foundation of China grants No.72171216 and 12231017, and the National Key R&D Program of China No.2022YFA1003803. Lin’s research is partially supported by National Natural Science Foundation of China grants No.12171310 and the Shanghai Natural Science Foundation No.20ZR1421800.

References

- Bahmani S, Raj B, Boufounos PT (2013) Greedy sparsity-constrained optimization. *Journal of Machine Learning Research* 14(25):807–841.
- Beck A, Eldar YC (2013) Sparsity constrained nonlinear optimization: optimality conditions and algorithms. *SIAM Journal on Optimization* 23(3):1480–1509.
- Bertsimas D, Cory-Wright R, Pauphilet J (2021) A unified approach to mixed-integer optimization problems with logical constraints. *SIAM Journal on Optimization* 31(3):2340–2367.
- Blumensath T, Davies ME (2008) Iterative thresholding for sparse approximations. *Journal of Fourier Analysis and Applications* 14(5):629–654.

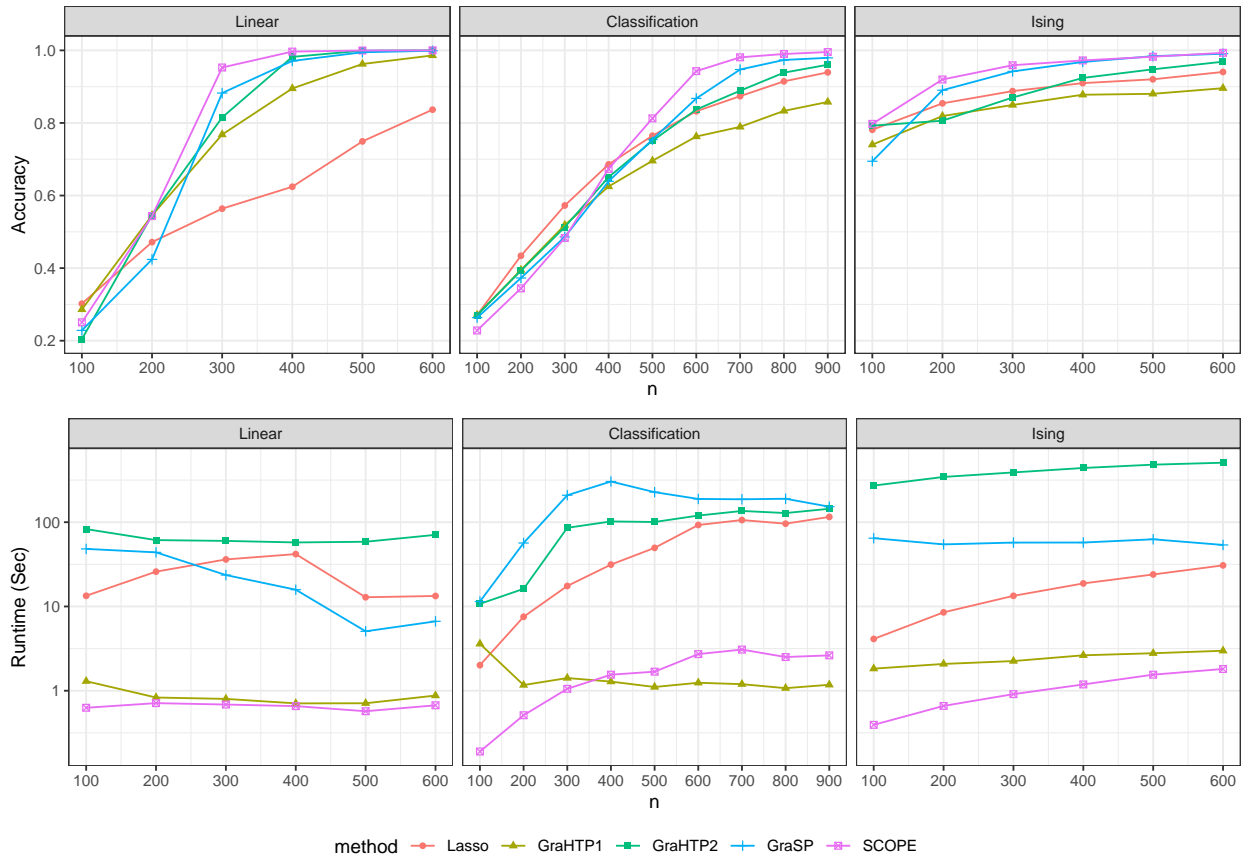


Figure 2 The accuracy (upper panel) and runtime (bottom panel) as the sample size increases from 100 with step size 100. All experiments were independently repeated 100 times. The y -axis for runtime is \log_{10} -transformed.

- Candes EJ, Romberg JK, Tao T (2006) Stable signal recovery from incomplete and inaccurate measurements. *Communications on Pure and Applied Mathematics: A Journal Issued by the Courant Institute of Mathematical Sciences* 59(8):1207–1223.
- Candes EJ, Tao T (2005) Decoding by linear programming. *IEEE Transactions on Information Theory* 51(12):4203–4215, URL <http://dx.doi.org/10.1109/TIT.2005.858979>.
- Diamond S, Boyd S (2016) CVXPY: a python-embedded modeling language for convex optimization. *Journal of Machine Learning Research* 17(83):1–5.
- Donoho DL (2006) Compressed sensing. *IEEE Transactions on Information Theory* 52(4):1289–1306.
- Foucart S (2011) Hard thresholding pursuit: an algorithm for compressive sensing. *SIAM Journal on Numerical Analysis* 49(6):2543–2563.
- Gurobi Optimization, LLC (2022) Gurobi optimizer reference manual. URL <https://www.gurobi.com>.
- Hazimeh H, Mazumder R (2020) Fast best subset selection: coordinate descent and local combinatorial optimization algorithms. *Operations Research* 68(5):1517–1537.
- Höfling H, Tibshirani R (2009) Estimation of sparse binary pairwise markov networks using pseudo-likelihoods. *Journal of Machine Learning Research* 10(32):883–906.
- Jain P, Tewari A, Kar P (2014) On iterative hard thresholding methods for high-dimensional M-estimation. *Advances in Neural Information Processing Systems* 27.
- Liu J, Ye J, Fujimaki R (2014) Forward-backward greedy algorithms for general convex smooth functions over a cardinality constraint. *International Conference on Machine Learning*, 503–511 (PMLR).
- Lokhov AY, Vuffray M, Misra S, Chertkov M (2018) Optimal structure and parameter learning of ising models. *Science advances* 4(3):e1700791.
- Needell D, Tropp JA (2009) CoSaMP: iterative signal recovery from incomplete and inaccurate samples. *Applied and Computational Harmonic Analysis* 26(3):301–321.
- Park MY, Hastie T (2007) L_1 -regularization path algorithm for generalized linear models. *Journal of the Royal Statistical Society: Series B (Statistical Methodology)* 69(4):659–677.
- Rigollet P (2012) Kullback-leibler aggregation and misspecified generalized linear models. *Annals of Statistics* 639–665.
- Santhanam NP, Wainwright MJ (2012) Information-theoretic limits of selecting binary graphical models in high dimensions. *IEEE Transactions on Information Theory* 58(7):4117–4134.
- Shalev-Shwartz S, Srebro N, Zhang T (2010) Trading accuracy for sparsity in optimization problems with sparsity constraints. *SIAM Journal on Optimization* 20(6):2807–2832, ISSN 1052-6234, 1095-7189.

- Shen J, Li P (2017) A tight bound of hard thresholding. *Journal of Machine Learning Research* 18(1):7650–7691, ISSN 1532-4435.
- Shen X, Pan W, Zhu Y (2012) Likelihood-based selection and sharp parameter estimation. *Journal of the American Statistical Association* 107(497):223–232.
- Tibshirani R (1996) Regression shrinkage and selection via the lasso. *Journal of the Royal Statistical Society: Series B (Statistical Methodology)* 58(1):267–288, ISSN 00359246.
- Tropp JA, Gilbert AC (2007) Signal recovery from random measurements via orthogonal matching pursuit. *IEEE Transactions on Information Theory* 53(12):4655–4666.
- Wainwright MJ (2019) *High-dimensional statistics: a non-asymptotic viewpoint* (Cambridge University Press).
- Wen C, Zhang A, Quan S, Wang X (2020) BeSS: an R package for best subset selection in linear, logistic and cox proportional hazards models. *Journal of Statistical Software* 94:1–24.
- Xue L, Zou H, Cai T (2012) Nonconcave penalized composite conditional likelihood estimation of sparse ising models. *Annals of Statistics* 40(3):1403–1429.
- Yuan X, Li P, Zhang T (2017) Gradient hard thresholding pursuit. *Journal of Machine Learning Research* 18:1–43.
- Yuan X, Liu B, Wang L, Liu Q, Metaxas DN (2020) Dual iterative hard thresholding. *Journal of Machine Learning Research* 21(152):1–50.
- Zhang C, Huang J (2008) The sparsity and bias of the lasso selection in high-dimensional linear regression. *Annals of Statistics* 36(4):1567–1594.
- Zhou S, Xiu N, Qi H (2021) Global and quadratic convergence of newton hard-thresholding pursuit. *Journal of Machine Learning Research* 45.
- Zhu J, Wen C, Zhu J, Zhang H, Wang X (2020) A polynomial algorithm for best-subset selection problem. *Proceedings of the National Academy of Sciences* 117(52):33117–33123.
- Zhu Z, Li X, Wang M, Zhang A (2022) Learning markov models via low-rank optimization. *Operations Research* 70(4):2384–2398.

Appendix A: Proof for Theoretical Results

A.1. Proof of Lemmas 1-2.

Proof of Lemma 1. For any \mathcal{A} and \mathbf{x} which satisfy $|\mathcal{A} \cup \text{supp}(\mathbf{x})| \leq k$, let $\mathcal{F} = \mathcal{A} \cup \text{supp}(\mathbf{x})$ and consider the set $\Omega_S = \{a \in \mathbb{R}^p \mid \text{supp}(a) \subseteq \mathcal{F}\}$. It is easy to see that Ω_S is a convex set. Because of f is m_k -RSC and M_k -RSS, for $\forall a, b \in \Omega_S$, $|\text{supp}(a - b)| \leq |\mathcal{F}| \leq k$, we have:

$$\frac{m_k}{2} \|a - b\|^2 \leq f(a) - f(b) - \nabla f(b)^\top [a - b] \leq \frac{M_k}{2} \|a - b\|^2.$$

Hence, we have the following:

$$\begin{aligned} f(a) &\leq f(b) + \nabla f(b)^\top (a - b) + \frac{M_k}{2} \|a - b\|^2, \\ f(a) &\geq f(b) + \nabla f(b)^\top (a - b) + \frac{m_k}{2} \|a - b\|^2. \end{aligned} \quad (32)$$

We can find that (32) are first order conditions for convexity of $\frac{M_k}{2} \|a\|^2 - f(a)$ and $f(a) - \frac{m_k}{2} \|a\|^2$ at Ω_S :

$$\begin{aligned} &[f(a) - \frac{m_k}{2} \|a\|^2] - [f(b) - \frac{m_k}{2} \|b\|^2] \geq \nabla [f(b) - \frac{m_k}{2} \|b\|^2]^\top (a - b) \\ \Leftrightarrow f(a) &\geq f(b) + \frac{m_k}{2} (\|a\|^2 - \|b\|^2) + [\nabla f(b) - m_k b]^\top (a - b) \\ \Leftrightarrow f(a) &\geq f(b) + \nabla f(b)^\top (a - b) + \frac{m_k}{2} (\|a\|^2 - \|b\|^2 - 2b^\top a + 2b^\top b) \\ \Leftrightarrow f(a) &\geq f(b) + \nabla f(b)^\top (a - b) + \frac{m_k}{2} \|a - b\|^2. \end{aligned}$$

Therefore, $f(a) - \frac{m_k}{2} \|a\|^2$ is convex at Ω_S , so does $\frac{M_k}{2} \|a\|^2 - f(a)$ similarly. Then, by second-order condition for convexity of the two functions, we have:

$$\nabla^2 [\frac{M_k}{2} \|a\|^2 - f(a)] \succeq 0 \text{ and } \nabla^2 [f(a) - \frac{m_k}{2} \|a\|^2] \succeq 0.$$

for any $a \in \Omega_{\mathcal{F}}$. In other words, we have $m_k I_{|\mathcal{F}|} \preceq \nabla^2 f(a) \preceq M_k I_{|\mathcal{F}|}$ for $\forall a \in \Omega_S$. Since $\nabla_{\mathcal{A}}^2 f(\mathbf{x})$ is a principle submatrix of $\nabla_{\mathcal{F}}^2 f(\mathbf{x})$, so we get the conclusion:

$$m_k I_{|\mathcal{A}|} \preceq \nabla_{\mathcal{A}}^2 f(\mathbf{x}) \preceq M_k I_{|\mathcal{A}|}.$$

Proof of Lemma 2. Denote $\mathcal{F} = \mathcal{A} \cup \mathcal{B}$, then

$$\nabla_{\mathcal{F}}^2 f(\mathbf{x}) = \begin{pmatrix} \nabla_{\mathcal{A}}^2 f(\mathbf{x}) & \nabla_{\mathcal{B}} \nabla_{\mathcal{A}} f(\mathbf{x}) \\ \nabla_{\mathcal{A}} \nabla_{\mathcal{B}} f(\mathbf{x}) & \nabla_{\mathcal{B}}^2 f(\mathbf{x}) \end{pmatrix}.$$

Let $X = \nabla_{\mathcal{F}}^2 f(\mathbf{x}) - \frac{M_k + m_k}{2} I_{|\mathcal{F}|}$, by Lemma 1, we have:

$$-\frac{M_k - m_k}{2} I_{|\mathcal{F}|} \preceq X \preceq \frac{M_k - m_k}{2} I_{|\mathcal{F}|}.$$

And we can get $X^\top X \preceq \left(\frac{M_k - m_k}{2}\right)^2 I_{|\mathcal{F}|}$, then $\forall u \in \mathbb{R}^{|\mathcal{F}|}$, $\|Xu\| = \sqrt{u^\top X^\top X u} \leq \sqrt{\left(\frac{M_k - m_k}{2}\right)^2 \|u\|^2} = \frac{M_k - m_k}{2} \|u\|$. Due to $\mathcal{A} \cap \mathcal{B} = \emptyset$, $\nabla_{\mathcal{A}} \nabla_{\mathcal{B}} f(\mathbf{x})$ is submatrix of X , and hence $\forall v \in \mathbb{R}^{|\mathcal{A}|}$, let $\tilde{v} = (0^\top, v^\top)^\top \in \mathbb{R}^{|\mathcal{F}|}$, we have:

$$\|\nabla_{\mathcal{A}} \nabla_{\mathcal{B}} f(\mathbf{x})v\| \leq \|X\tilde{v}\| \leq \frac{M_k - m_k}{2} \|\tilde{v}\| = \frac{M_k - m_k}{2} \|v\|.$$

For $\forall w \in \mathbb{R}^{|\mathcal{B}|}$, Cauchy-Schwartz inequality implies:

$$w^\top \nabla_{\mathcal{A}} \nabla_{\mathcal{B}} f(\mathbf{x})v \leq \|w\| \cdot \|\nabla_{\mathcal{A}} \nabla_{\mathcal{B}} f(\mathbf{x})v\| \leq \frac{M_k - m_k}{2} \|w\| \|v\|.$$

A.2. Proof of Proposition 1

Proof of Proposition 1 Let $\phi_k(\mathbf{x}_i) := \mathbb{P}(\mathbf{x}_{ik} | \mathbf{x}_{i1}, \dots, \mathbf{x}_{ik-1}, \mathbf{x}_{ik+1}, \dots, \mathbf{x}_{ip}) = \frac{1}{1 + \exp(-2 \sum_{l:l \neq k} \mathbf{x}_{il} \theta_{kl})}$, we can attain the differentiations of $f(\boldsymbol{\theta})$ by simple algebra:

$$\begin{aligned} (\nabla f)_{kl} &:= \frac{\partial f(\boldsymbol{\theta})}{\partial \theta_{kl}} = -\frac{2}{n} \sum_{i=1}^n \mathbf{x}_{ik} \mathbf{x}_{il} (1 - \phi_k(\mathbf{x}_i) + 1 - \phi_l(\mathbf{x}_i)), \\ (\nabla^2 f)_{kl;vw} &:= \frac{\partial^2 f(\boldsymbol{\theta})}{\partial \theta_{kl} \partial \theta_{vw}} = \begin{cases} \frac{4}{n} \sum_{i=1}^n (1 - \phi_k(\mathbf{x}_i)) \phi_k(\mathbf{x}_i) + (1 - \phi_l(\mathbf{x}_i)) \phi_l(\mathbf{x}_i) & \text{if } k = v, l = w \\ \frac{4}{n} \sum_{i=1}^n \mathbf{x}_{il} \mathbf{x}_{iw} (1 - \phi_k(\mathbf{x}_i)) \phi_k(\mathbf{x}_i) & \text{if } k = v, l \neq w \\ 0 & \text{other} \end{cases} \end{aligned}$$

Let \mathbf{u} be an arbitrary vector with dimension $p \times p$ satisfying $|\text{supp}(\mathbf{u})| \leq 3s$ and $\|\mathbf{u}\| = 1$. For any $k \in [p]$, denote $W_k := \text{diag}\{4(1 - \phi_k(\mathbf{x}_1))\phi_k(\mathbf{x}_1), \dots, 4(1 - \phi_k(\mathbf{x}_n))\phi_k(\mathbf{x}_n)\}$ and $\text{Tr}(W_k)$ as its trace. And define subvector of \mathbf{u} that has length $p - 1$ as $\mathbf{u}_{-k} := (\mathbf{u}_{kl})$ for $l \in [p]$ and $l \neq k$, then \mathbf{u}_{-k} satisfies $|\text{supp}(\mathbf{u}_{-k})| \leq \min\{3s, p - 1\}$. Then, we have

$$\begin{aligned} &\mathbf{u}^\top (\nabla^2 f) \mathbf{u} \\ &= \sum_{k=1}^p \sum_{\substack{v \neq k \\ w \neq k}} \mathbf{u}_{kv} \mathbf{u}_{kw} \frac{4}{n} \sum_{i=1}^n (\mathbf{x}_{iv} \mathbf{x}_{iw} (1 - \phi_k(\mathbf{x}_i)) \phi_k(\mathbf{x}_i) + \mathbf{I}(v = w) (1 - \phi_v(\mathbf{x}_i)) \phi_v(\mathbf{x}_i)) \\ &= \sum_{k=1}^p \sum_{\substack{v \neq k \\ w \neq k}} \mathbf{u}_{kv} \mathbf{u}_{kw} \left(\frac{1}{n} \mathbf{X}^\top W_k \mathbf{X} + \frac{1}{n} \text{diag}\{\text{Tr}(W_1), \dots, \text{Tr}(W_p)\} \right)_{vw} \\ &= \sum_{k=1}^p \mathbf{u}_{-k}^\top \left(\frac{1}{n} \mathbf{X}^\top W_k \mathbf{X} + \frac{1}{n} \text{diag}\{\text{Tr}(W_1), \dots, \text{Tr}(W_p)\} \right)_{-k, -k} \mathbf{u}_{-k} \\ &\leq \sum_{k=1}^p \mathbf{u}_{-k}^\top \left(\frac{1}{n} \mathbf{X}^\top \mathbf{X} + \mathbf{I}_p \right)_{-k, -k} \mathbf{u}_{-k} \leq (1 + M_{3s}) \sum_{k=1}^p \mathbf{u}_{-k}^\top \mathbf{u}_{-k} \leq (1 + M_{3s}) \|\mathbf{u}\|, \end{aligned}$$

where the second inequality leverages Condition (C1). Thus, $f(\cdot)$ is $(1 + M_{3s})$ -RSS.

Note that Δ satisfies $\Delta \leq \phi_k(\mathbf{x}_i)(1 - \phi_k(\mathbf{x}_i))$ for any $k \in [p]$. Then, with Conditions (C1) and (C2), we can get $\mathbf{u}^\top (\nabla^2 f) \mathbf{u} \geq 8\Delta(1 + m_{3s})$ by following the similar procedure for deriving its upper bound. So, $f(\cdot)$ is $8\Delta(1 + m_{3s})$ -RSC.

Appendix B: Parameter estimation analysis

B.1. Case I: with RIP-type condition

THEOREM 7. *Following Assumptions and notations in Theorem 3, there exists a constant $\delta_3 > 0$ such that the ℓ_2 -error of $\boldsymbol{\theta}^t$ is upper bounded by*

$$\|\boldsymbol{\theta}^t - \boldsymbol{\theta}^*\|^2 \leq \frac{\delta_3}{m_{3s}} \delta_1^{-t} |f(\boldsymbol{\theta}^0) - f(\boldsymbol{\theta}^*)|, \quad (33)$$

if $\boldsymbol{\theta}^t$ is not the oracle solution.

Proof of Theorem 7 Let $\mathcal{A}^t = \text{supp}\{\boldsymbol{\theta}^t\}$, $\mathcal{A}_1^t = \mathcal{A}^t \cap \mathcal{A}^*$, and $\mathcal{I}_1^t = (\mathcal{A}^t)^c \cap \mathcal{A}^*$, then following the immediate results in Lemma 3, we have:

$$\begin{aligned} \|\boldsymbol{\theta}^t - \boldsymbol{\theta}^*\| &\stackrel{(11)}{\leq} m^{-1} \|\mathbf{d}_{\mathcal{A}^t}^*\| + \left(\frac{v}{m} + 1\right) \|\boldsymbol{\theta}_{\mathcal{I}_1^t}^*\| \\ &\leq \left(\frac{\sqrt{sc}}{m} + \frac{v}{m} + 1\right) \|\boldsymbol{\theta}_{\mathcal{I}_1^t}^*\| \\ &\stackrel{(5)}{\leq} \frac{\left(\frac{\sqrt{sc}}{m} + \frac{v}{m} + 1\right) \sqrt{|f(\boldsymbol{\theta}^t) - f(\boldsymbol{\theta}^*)|}}{\sqrt{\frac{m}{2} - \sqrt{2sc}}}, \end{aligned}$$

where the second inequality results from Assumption 2. Furthermore, according to the result of Theorem 2, we have

$$\begin{aligned} \|\boldsymbol{\theta}^t - \boldsymbol{\theta}^*\| &\leq \frac{\left(\frac{\sqrt{sc}}{m} + \frac{v}{m} + 1\right) \sqrt{\frac{|f(\boldsymbol{\theta}^0) - f(\boldsymbol{\theta}^*)|}{m\delta_1^t}}}{\sqrt{\frac{1}{2} - \frac{\sqrt{2sc}}{m}}} \\ &\leq \frac{(0.15x + 1.0215) \sqrt{\frac{|f(\boldsymbol{\theta}^0) - f(\boldsymbol{\theta}^*)|}{m\delta_1^t}}}{\sqrt{\left(\frac{1}{2} - \sqrt{2}(0.5215 - 0.35x)\right)}} \\ &\leq 2.31 \sqrt{\frac{|f(\boldsymbol{\theta}^0) - f(\boldsymbol{\theta}^*)|}{m\delta_1^t}}, \end{aligned}$$

where x in the second inequality is defined as $x := M/m$, and the last inequality follows from $x \in [1, 1.49]$ implied by Assumption 2.

B.2. Case II: without RIP-type condition

THEOREM 8. *Following the same assumptions and notations in Theorem 5, ℓ_2 -error of $\boldsymbol{\theta}^t$ is upper bounded by*

$$\|\boldsymbol{\theta}^t - \boldsymbol{\theta}^*\| \leq \sqrt{\frac{2(1 - \delta_4)^t}{m_{s+s^*}} \max\{f(\boldsymbol{\theta}^0) - f(\boldsymbol{\theta}^*), 0\}} + \frac{2\sqrt{s+s^*}}{m_{s+s^*}} \|\nabla f(\boldsymbol{\theta}^*)\|_\infty. \quad (34)$$

Proof of Theorem 8. Without the loss of generality, this proof adopts the notations used in proving Theorem 5. It is easily seen that

$$\begin{aligned} 0 &\geq f(\boldsymbol{\theta}^*) - f(\hat{\boldsymbol{\theta}}) + (\hat{\boldsymbol{\theta}} - \boldsymbol{\theta}^*)^\top \mathbf{d}^* + \frac{m}{2} \|\hat{\boldsymbol{\theta}} - \boldsymbol{\theta}^*\|^2 \\ &\geq \frac{m}{2} \|\hat{\boldsymbol{\theta}} - \boldsymbol{\theta}^*\|^2 - \|\mathbf{d}_{\mathcal{I}_2^C}^*\| \|\hat{\boldsymbol{\theta}} - \boldsymbol{\theta}^*\| + f(\boldsymbol{\theta}^*) - f(\hat{\boldsymbol{\theta}}) \\ &= \frac{m}{2} \left(\|\hat{\boldsymbol{\theta}} - \boldsymbol{\theta}^*\| - \frac{\|\mathbf{d}_{\mathcal{I}_2^C}^*\|}{m}\right)^2 - \frac{\|\mathbf{d}_{\mathcal{I}_2^C}^*\|^2}{2m} + f(\boldsymbol{\theta}^*) - f(\hat{\boldsymbol{\theta}}). \end{aligned}$$

Considering the first case that $f(\boldsymbol{\theta}^*) - f(\hat{\boldsymbol{\theta}}) \geq 0$, we can derive $\|\hat{\boldsymbol{\theta}} - \boldsymbol{\theta}^*\| \leq \frac{2}{m} \|\mathbf{d}_{\mathcal{I}_2^C}^*\|$. Moreover, due to $|\mathcal{I}_2^C| \leq s + s^*$, we have $\frac{2}{m} \|\mathbf{d}_{\mathcal{I}_2^C}^*\| \leq \frac{2\sqrt{s+s^*}}{m} \|\mathbf{d}^*\|_\infty$. Thus, it leads to $\|\hat{\boldsymbol{\theta}} - \boldsymbol{\theta}^*\| \leq \frac{2\sqrt{s+s^*}}{m} \|\mathbf{d}^*\|_\infty$, which coincides with (34).

On the other hand, when $f(\boldsymbol{\theta}^*) - f(\hat{\boldsymbol{\theta}}) < 0$, we can get

$$\begin{aligned}
& \|\hat{\boldsymbol{\theta}} - \boldsymbol{\theta}^*\| \\
& \leq \frac{1}{m} \|\mathbf{d}_{\mathcal{T}_2^c}^*\| + \frac{1}{m} \sqrt{\|\mathbf{d}_{\mathcal{T}_2^c}^*\|^2 - 2m(f(\boldsymbol{\theta}^*) - f(\hat{\boldsymbol{\theta}}))} \\
& \leq \frac{2}{m} \|\mathbf{d}_{\mathcal{T}_2^c}^*\| + \sqrt{\frac{2}{m} \sqrt{f(\hat{\boldsymbol{\theta}}) - f(\boldsymbol{\theta}^*)}} \\
& \leq \frac{2\sqrt{s+s^*}}{m} \|\mathbf{d}^*\|_\infty \\
& \quad + \sqrt{\frac{2}{m} \sqrt{(1-\delta_4)^t \max\{f(\boldsymbol{\theta}^0) - f(\boldsymbol{\theta}^*), 0\}}}
\end{aligned}$$

where the last inequality follows from recursively applying Theorem 5 and the fact that $f(\boldsymbol{\theta}^0) \geq f(\boldsymbol{\theta}^1) \geq \dots \geq f(\boldsymbol{\theta}^{t-1}) \geq f(\boldsymbol{\theta}^t) =: f(\hat{\boldsymbol{\theta}})$.

Appendix C: Selection of k_{\max}

From Algorithm 1, k_{\max} trade-offs the number of splicing iterations and the number of splicing operators with each splicing iteration. Specifically, a large k_{\max} enlarges the number of splicing but reduces the number of splicing iterations; and vice versa. Although the proof of Theorem 1 requires k_{\max} to be the true size of active set s , we can still get a similar result when k_{\max} is smaller than s . We compare the results with different k_{\max} to see this.

The way of data generation is completely the same as the experiments in Section 6.2. The results in Figure 3 show that the performance of our algorithm is insensitive to k_{\max} , and a medium-sized k_{\max} makes the algorithm more computationally efficient. Thus, $k_{\max} = 5$ maybe a rule-of-thumb setting.

We provide an intuitive explanation of the benefits of selecting a moderate-sized tuning parameter. In terms of statistical properties, the proof of Theorem 1 highlights that setting $k_{\max} = s$ primarily addresses the scenario where none of the effective variables are selected. However, this situation is rare in practice, especially when we have well-initialized values. In terms of computation, our previous discussion on k_{\max} reveals that choosing a large k_{\max} significantly increases the number of splicing operators. Unfortunately, this does not result in a substantial reduction in the number of splicing iterations, ultimately leading to a significant increase in computational time.

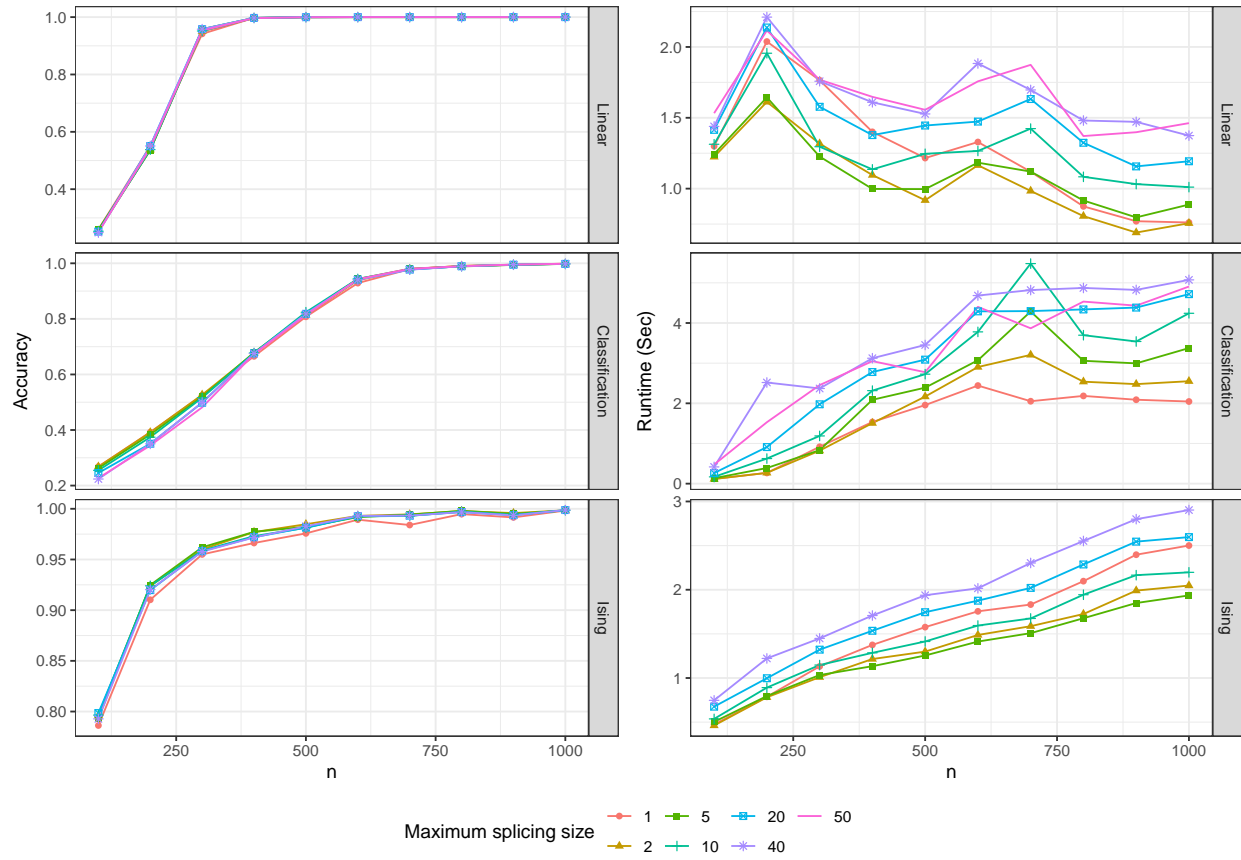


Figure 3 The mean of accuracy and runtime as sample size increases for different hyper-parameter k_{max} . The experiment was independently repeated 20 times.